The Astrophysical Journal, 850:122 (21pp), 2017 December 1 https://doi.org/10.3847/1538-4357/aa9276

Electron-impact Multiple-ionization Cross Sections for Atoms and Ions of Helium through Zinc

M. Hahn[1], A. Müller[2], and D. W. Savin[1]
[1] Columbia Astrophysics Laboratory, Columbia University, 550 West 120th Street, New York, NY 10027, USA; mhahn@astro.columbia.edu
[2] Institut für Atom- und Molekülphysik, Justus-Liebig-Universität Giessen, Leihgesterner Weg 217, D-35392 Giessen, Germany
Received 2017 August 2; revised 2017 September 29; accepted 2017 October 6; published 2017 November 22

Abstract

We compiled a set of electron-impact multiple-ionization (EIMI) cross section for astrophysically relevant ions. EIMIs can have a significant effect on the ionization balance of non-equilibrium plasmas. For example, it can be important if there is a rapid change in the electron temperature or if there is a non-thermal electron energy distribution, such as a kappa distribution. Cross section for EIMI are needed in order to account for these processes in plasma modeling and for spectroscopic interpretation. Here, we describe our comparison of proposed semiempirical formulae to available experimental EIMI cross-section data. Based on this comparison, we interpolated and extrapolated fitting parameters to systems that have not yet been measured. A tabulation of the fit parameters is provided for 3466 EIMI cross sections and the associated Maxwellian plasma rate coefficients. We also highlight some outstanding issues that remain to be resolved.

Key words: atomic data – atomic processes – techniques: spectroscopic

Supporting material: figure set, machine-readable tables

1. Introduction

Collisionally ionized plasmas are those formed by electron-impact ionization (EII). Such plasmas are common in astrophysical sources, such as stars, supernova remnants, galaxies, and galaxy clusters. Modeling the emission from these objects requires knowing the charge state distribution (CSD) within the plasma, which is set by the ionization and recombination rates (Bryans et al. 2006, 2009).

Electron-impact multiple ionization (EIMI) is the EII process in which a single electron–ion collision results in the ejection of multiple electrons. In most previous works, EIMI has been ignored. For plasmas near thermal equilibrium, the multiple-ionization rates for a given charge state are insignificant at the temperatures where that charge state is most abundant. However, EIMI can be important in dynamic systems where ions are suddenly exposed to higher electron temperatures (Müller 1986; Hahn & Savin 2015a). For this reason, EIMI may be important for studies of solar flares (Reale & Orlando 2008; Bradshaw & Klimchuk 2011), nanoflare coronal heating (Hahn & Savin 2015a), supernova remnants (Patnaude et al. 2009), and merging galaxy clusters (Akahori & Yoshikawa 2010). EIMI can also have a significant effect on the CSD for plasmas with a non-thermal electron energy distribution. For such plasmas, there is a substantial population of electrons in the high-energy tail of the distribution that lie above the EIMI threshold (Hahn & Savin 2015b). Thus, EIMI is relevant to the modeling of astrophysical systems where such non-thermal distributions are present.

Due in part to the lack of data, EIMI has largely been ignored, despite its relevance to astrophysical models. One reason for the lack of EIMI data is that theoretical calculations for EIMI are very challenging. There are at least four particles whose interactions must be accounted for: the ion, incident electron, and two or more ejected electrons (Berakdar 1996; Müller 2005; Götz et al. 2006). This means that there are at least three electrons in the continuum. Because of these difficulties, theoretical calculations have mainly been performed for simple systems (e.g., Defrance et al. 2000; Pindzola et al. 2009, 2010, 2011), though recent work is attempting to extend these calculations to more complex systems (e.g., Pindzola & Loch 2017).

Most EIMI cross sections are based on experimental measurements. For astrophysical applications, EIMI data are needed for nearly all of the charge states of all elements from He–Zn. However, it is not possible for experiments to measure all of these data. In order to estimate cross sections for unmeasured systems, various semiempirical formulae have been proposed.

Here, we produced a database of EIMI cross sections for astrophysics. In order to generate this database, we compared measurements of EIMI cross sections to predictions using the proposed semiempirical formulae. Table 1 gives the references for all of the experimental data sources that we consulted. Based on this comparison, we selected the semiempirical scheme that worked best for a given isoelectronic sequence and EIMI process (e.g., double, triple, etc.) and then used that scheme to generate EIMI cross sections for the unmeasured systems. The procedures are described below in Section 2, and their application to each isoelectronic sequence is discussed in Section 3. The main results of this work are the tabulated cross-section parameters, which are available in machine-readable table format, a selection of which is illustrated in Table 2. Section 4 concludes with a brief summary of the state of the EIMI data and avenues for future improvements. A tabulation of Maxwellian EIMI plasma rate coefficients and an extensive figure set (Figure 17) comparing our recommended cross sections to experimental measurements are given in the appendices.

2. Electron-impact Multiple-ionization Cross sections

EIMI can proceed via several different processes (Müller 2008). These processes can be divided into the categories of direct ionization (DI) and indirect processes such as excitation–multiple-autoionization (EMA), ionization–autoionization (IA), and multiple-ionization–multiple-autoionization (MIMA). This classification is oversimplified, as even direct multiple ionization can be broken down into a sequence of processes. For example,

Table 1
Experimental EIMI Data Sources

Order	Sequence	Atom or Ion	Reference	Comment
2	He	He^{0+}	Shah et al. (1988)	…
2	He	He^{0+}	Rejoub et al. (2002)	…
2	He	Li^{1+}	Peart & Dolder (1969)	…
2	Li	Li^{0+}	Jalin et al. (1973)	…
2	Li	Li^{0+}	Huang et al. (2002)	…
2	Li	C^{3+}	Westermann et al. (1999)	Data from private communication
2	Li	N^{4+}	Westermann et al. (1999)	Data from private communication
2	Be	B^{1+}	Scheuermann et al. (2001, private communication)	Reported in Shevelko et al. (2005)
2	Be	C^{2+}	Westermann et al. (1999)	Data from private communication
2	Be	N^{3+}	Westermann et al. (1999)	Data from private communication
2	Be	O^{4+}	Westermann et al. (1999)	Data from private communication
2	Be	Ne^{6+}	Duponchelle et al. (1997)	…
2	B	C^{1+}	Zambra et al. (1994)	…
2	B	C^{1+}	Westermann et al. (1999)	Data from private communication
2	B	C^{1+}	Lecointre et al. (2013)	…
2	B	N^{2+}	Westermann et al. (1999)	Data from private communication
2	B	O^{3+}	Westermann et al. (1999)	Data from private communication
2	B	Ne^{5+}	Duponchelle et al. (1997)	…
2	C	N^{1+}	Zambra et al. (1994)	…
2	C	N^{1+}	Lecointre et al. (2013)	…
2	C	O^{2+}	Westermann et al. (1999)	Data from private communication
2	C	Ne^{4+}	Tinschert (1989)	Data from private communication. See also Shevelko et al. (2005)
2	N	O^{1+}	Zambra et al. (1994)	…
2	N	O^{1+}	Westermann et al. (1999)	Data from private communication
2	N	O^{1+}	Lecointre et al. (2013)	…
2	N	Ne^{3+}	Tinschert (1989)	Data from private communication. See also Shevelko et al. (2005)
2	N	Ar^{11+}	Zhang et al. (2002)	…
2	O	O^{0+}	Ziegler et al. (1982b)	…
2	O	O^{0+}	Thompson et al. (1995)	…
2	O	F^{1+}	Zambra et al. (1994)	…
2	O	Ne^{2+}	Tinschert (1989)	Data from private communication. See also Shevelko et al. (2005)
2	O	Ar^{10+}	Zhang et al. (2002)	…
2	F	Ne^{1+}	Tinschert (1989)	Data from private communication. See also Shevelko et al. (2005)
2	F	Ne^{1+}	Zambra et al. (1994)	…
2	F	Al^{4+}	Steidl et al. (1999)	Data from private communication
2	F	Ar^{9+}	Zhang et al. (2002)	…
2	Ne	Ne^{0+}	Schram et al. (1966)	…
2	Ne	Ne^{0+}	Krishnakumar & Srivastava (1988)	…
2	Ne	Ne^{0+}	Lebius et al. (1989)	…
2	Ne	Ne^{0+}	Almeida et al. (1995)	…
2	Ne	Ne^{0+}	Rejoub et al. (2002)	…
2	Ne	Na^{1+}	Hirayama et al. (1986)	See NIFS database at https://dbshino.nifs.ac.jp
2	Ne	Al^{3+}	Steidl et al. (1999)	Data from private communication
2	Ne	Ar^{8+}	Zhang et al. (2002)	…
2	Na	Na^{0+}	Tate & Smith (1934)	…
2	Na	Al^{2+}	Steidl et al. (1999)	Data from private communication
2	Na	Ar^{7+}	Tinschert et al. (1989)	…
2	Na	Ar^{7+}	Rachafi et al. (1991)	…
2	Na	Ar^{7+}	Zhang et al. (2002)	…
2	Mg	Mg^{0+}	McCallion et al. (1992b)	…
2	Mg	Mg^{0+}	Boivin & Srivastava (1998)	…
2	Mg	Al^{1+}	Steidl et al. (1999)	Data from private communication
2	Mg	Ar^{6+}	Tinschert et al. (1989)	…
2	Mg	Ar^{6+}	Zhang et al. (2002)	…
2	Al	Ar^{5+}	Tinschert et al. (1989)	…
2	A1	Fe^{13+}	Hahn et al. (2013)	…
2	A1	Ni^{15+}	Cherkani-Hassani et al. (2001)	…
2	Si	Si^{0+}	Freund et al. (1990)	…
2	Si	Ar^{4+}	Müller et al. (1985)	…
2	Si	Fe^{12+}	Hahn et al. (2011b)	…
2	Si	Ni^{14+}	Cherkani-Hassani et al. (1999)	…
2	P	P^{0+}	Freund et al. (1990)	…

Table 1
(Continued)

Order	Sequence	Atom or Ion	Reference	Comment
2	P	Ar^{3+}	Müller & Frodl (1980)	…
2	P	Ar^{3+}	Tinschert et al. (1989)	…
2	P	Fe^{11+}	Hahn et al. (2011a)	…
2	P	Ni^{13+}	Cherkani-Hassani et al. (2001)	…
2	S	S^{0+}	Ziegler et al. (1982a)	…
2	S	S^{0+}	Freund et al. (1990)	…
2	S	Ar^{2+}	Müller & Frodl (1980)	…
2	S	Ar^{2+}	Tinschert et al. (1989)	…
2	S	Ti^{6+}	Hartenfeller et al. (1998)	See also Shevelko et al. (2006)
2	S	Ni^{12+}	Cherkani-Hassani et al. (1999)	…
2	Cl	Cl^{0+}	Freund et al. (1990)	…
2	Cl	Ar^{1+}	Müller & Frodl (1980)	…
2	Cl	Ar^{1+}	Müller et al. (1985)	…
2	Cl	Ar^{1+}	Belic et al. (2010)	…
2	Cl	Ti^{5+}	Hartenfeller et al. (1998)	See also Shevelko et al. (2006)
2	Cl	Fe^{9+}	Hahn et al. (2012)	…
2	Cl	Ni^{11+}	Cherkani-Hassani et al. (2001)	…
2	Ar	Ar^{0+}	Schram (1966)	…
2	Ar	Ar^{0+}	Krishnakumar & Srivastava (1988)	…
2	Ar	Ar^{0+}	Syage (1991)	…
2	Ar	Ar^{0+}	McCallion et al. (1992a)	…
2	Ar	Ar^{0+}	Straub et al. (1995)	…
2	Ar	Ar^{0+}	Rejoub et al. (2002)	…
2	Ar	K^{1+}	Hirayama et al. (1986)	See NIFS database at https://dbshino.nifs.ac.jp
2	Ar	Ti^{4+}	Hartenfeller et al. (1998)	See also Shevelko et al. (2006)
2	Ar	Ni^{10+}	Cherkani-Hassani et al. (1999)	…
2	K	Ti^{3+}	Hartenfeller et al. (1998)	See also Shevelko et al. (2006)
2	Ca	Sc^{1+}	Jacobi et al. (2005)	…
2	Ca	Ti^{2+}	Hartenfeller et al. (1998)	See also Shevelko et al. (2006)
2	Ca	Fe^{6+}	Stenke et al. (1999)	See also Shevelko et al. (2006)
2	Sc	Ti^{l+}	Hartenfeller et al. (1998)	See also Shevelko et al. (2006)
2	Sc	Fe^{5+}	Stenke et al. (1999)	See also Shevelko et al. (2006)
2	Ti	Fe^{4+}	Stenke et al. (1999)	See also Shevelko et al. (2006)
2	Ti	Ni^{6+}	Stenke et al. (1995)	See also Shevelko et al. (2006)
2	V	Fe^{3+}	Stenke et al. (1999)	See also Shevelko et al. (2006)
2	V	Ni^{5+}	Stenke et al. (1995)	See also Shevelko et al. (2006)
2	Cr	Ni^{4+}	Stenke et al. (1995)	See also Shevelko et al. (2006)
2	Mn	Fe^{1+}	Stenke et al. (1999)	See also Shevelko et al. (2006)
2	Mn	Ni^{3+}	Stenke et al. (1995)	See also Shevelko et al. (2006)
2	Fe	Fe^{0+}	Shah et al. (1993)	…
2	Fe	Ni^{2+}	Stenke et al. (1995)	See also Shevelko et al. (2006)
2	Co	Ni^{1+}	Stenke et al. (1995)	See also Shevelko et al. (2006)
2	Cu	Cu^{0+}	Freund et al. (1990)	…
2	Cu	Cu^{0+}	Bolorizadeh et al. (1994)	…
2	Zn	…	…	…
3	Li	Li^{0+}	Huang et al. (2003)	…
3	B	C^{l+}	Westermann et al. (1999)	Data from private communication
3	B	C^{1+}	Lecointre et al. (2013)	…
3	B	N^{2+}	Westermann et al. (1999)	Data from private communication
3	B	O^{3+}	Westermann et al. (1999)	Data from private communication
3	C	N^{1+}	Lecointre et al. (2013)	…
3	C	O^{2+}	Westermann et al. (1999)	Data from private communication
3	N	O^{1+}	Westermann et al. (1999)	Data from private communication
3	N	O^{1+}	Lecointre et al. (2013)	…
3	F	Ne^{1+}	Tinschert (1989)	Data from private communication
3	F	Ne^{1+}	…	Unpublished data from E. Salzborn's group
3	Ne	Ne^{0+}	Schram et al. (1966)	…
3	Ne	Ne^{0+}	Krishnakumar & Srivastava (1988)	…
3	Ne	Ne^{0+}	Lebius et al. (1989)	…
3	Ne	Ne^{0+}	Almeida et al. (1995)	…
3	Ne	Ne^{0+}	Rejoub et al. (2002)	…
3	Ne	Al^{3+}	Steidl et al. (1999)	Data from private communication
3	Na	Al^{2+}	Steidl et al. (1999)	Data from private communication

Table 1
(Continued)

Order	Sequence	Atom or Ion	Reference	Comment
3	Mg	Mg^{0+}	McCallion et al. (1992b)	…
3	Mg	Mg^{0+}	Boivin & Srivastava (1998)	…
3	Mg	Al^{1+}	Steidl et al. (1999)	Data from private communication
3	S	S^{0+}	Ziegler et al. (1982a)	…
3	S	Ar^{2+}	Müller & Frodl (1980)	…
3	S	Ni^{12+}	Cherkani-Hassani et al. (1999)	…
3	Cl	Ar^{1+}	Müller & Frodl (1980)	…
3	Cl	Ar^{1+}	Belic et al. (2010)	…
3	Ar	Ar^{0+}	Schram (1966)	…
3	Ar	Ar^{0+}	Krishnakumar & Srivastava (1988)	…
3	Ar	Ar^{0+}	Syage (1991)	…
3	Ar	Ar^{0+}	McCallion et al. (1992a)	…
3	Ar	Ar^{0+}	Almeida et al. (1994)	…
3	Ar	Ar^{0+}	Straub et al. (1995)	…
3	Ar	Ar^{0+}	Rejoub et al. (2002)	…
3	K	Ti^{3+}	Hartenfeller et al. (1998)	…
3	Ca	Sc^{1+}	Jacobi et al. (2005)	…
3	Ca	Ti^{2+}	Hartenfeller et al. (1998)	…
3	Sc	Ti^{1+}	Hartenfeller et al. (1998)	…
3	Fe	Fe^{0+}	Shah et al. (1993)	…
3	Cu	Cu^{0+}	Bolorizadeh et al. (1994)	…
4	C	N^{1+}	Lecointre et al. (2013)	…
4	N	O^{1+}	Westermann et al. (1999)	Data from private communication
4	N	O^{1+}	Lecointre et al. (2013)	…
4	Ne	Ne^{0+}	Schram et al. (1966)	…
4	Ne	Ne^{0+}	Krishnakumar & Srivastava (1988)	…
4	Ne	Ne^{0+}	Lebius et al. (1989)	…
4	Ne	Ne^{0+}	Almeida et al. (1995)	…
4	Ne	Ne^{0+}	Rejoub et al. (2002)	…
4	Mg	Mg^{0+}	McCallion et al. (1992b)	…
4	Mg	Al^{1+}	Steidl et al. (1999)	Data from private communication
4	S	S^{0+}	Ziegler et al. (1982a)	…
4	Cl	Ar^{1+}	Müller & Frodl (1980)	…
4	Cl	Ar^{1+}	Belic et al. (2010)	…
4	Ca	Sc^{1+}	Jacobi et al. (2005)	…
4	Sc	Ti^{1+}	Hartenfeller et al. (1998)	…
4	Cu	Cu^{0+}	Bolorizadeh et al. (1994)	…
5	Ne	Ne^{0+}	Schram et al. (1966)	…
5	Ne	Ne^{0+}	Almeida et al. (1995)	…
5	Cl	Ar^{1+}	Belic et al. (2010)	…
5	Ar	Ar^{0+}	Schram (1966)	…
5	Ar	Ar^{0+}	McCallion et al. (1992a)	…
5	Ar	Ar^{0+}	Almeida et al. (1994)	…
5	Ca	Sc^{1+}	Jacobi et al. (2005)	…
5	Cu	Sc^{1+}	Bolorizadeh et al. (1994)	…
6	Cl	Ar^{1+}	Belic et al. (2010)	…
6	Ar	Ar^{0+}	Schram (1966)	…
6	Ar	Ar^{0+}	Almeida et al. (1994)	…
7	Cl	Ar^{1+}	Belic et al. (2010)	…
7	Ar	Ar^{0+}	Schram (1966)	…

DI has often been considered to proceed via two-step mechanisms called TS1 and TS2 (Gryziński 1965). In TS1, the incident electron collides with and removes one electron, and then that previously bound electron collides with and removes another electron. In TS2, the incident electron collides with and removes both bound electrons sequentially. Recently, Jonauskas et al. (2014) extended this picture to include further processes, such as ionization–excitation–ionization and excitation–ionization–ionization. It is difficult to distinguish these processes in total cross-section measurements, although differential cross-section experiments can provide some information (e.g., Lahmam-Bennani et al. 2010).

We found that nearly all of the existing EIMI cross-section measurements can be adequately represented as a sum of DI and IA cross sections. The relative contribution of these processes depends on the isoelectronic sequence and the charge state. For example, the double ionization of ions in low-charge states is dominated by DI, while for more highly charged ions, the IA

Table 2
Fitting Formulae for EIMI Cross Sections

Z	q_i	q_f	Equation	$E_{\rm th}$	f	p_0	p_1	p_2	p_3	p_4
2	0	2	7	79.0052	1	2.6	6.501	1.743	−19.656	11.647
3	0	2	2	81.0318	1	5.8	0	0	0	0
3	0	3	1	203.486	0.00312	6.3	3	1.2	1	0
3	1	3	7	198.094	1	2.6	6.501	1.743	−19.656	11.647
4	0	2	2	27.5339	1	1.8	0	0	0	0
4	0	2	3	123.63	0.9999	3.6	4.5	0	0	0
4	1	3	2	172.107	1	12	0	0	0	0
4	2	4	7	371.615	1	2.6	6.501	1.743	−19.656	11.647

(This table is available in its entirety in machine-readable form.)

process dominates (e.g., Müller & Frodl 1980; Cherkani-Hassani et al. 2001; Hahn et al. 2011a). Although other processes such as EMA have been identified in some measurements (Müller et al. 1988), incorporating these effects into our representations of the cross sections would be cumbersome as there are insufficient data upon which to base an interpolation. Fortunately, the resulting cross-section errors are usually of little impact. Additionally, because of the strong dependence of the DI cross section on the EIMI energy threshold, the DI of a given number of electrons is greatest for the outermost subshells and is negligible for the inner subshells. Hence, we neglect the direct EIMI of the inner subshells except for a few cases of high-order EIMI, where the cross section for the DI of a small number of inner-shell electrons followed by MIMA can be similar in magnitude to that for the DI of a larger number of electrons from the outermost shells.

2.1. Fitting Formulae

In order to represent the EIMI cross sections, we use various semiempirical formulae. Direct EIMI can be described by (Shevelko & Tawara 1995a, 1995b; Bélenger et al. 1997)

$$\sigma_{\rm D} = f\frac{p_0 {p_1}^{p_2}}{(E_{\rm th}/E_{\rm Ryd})^2}\left(\frac{u+1}{u}\right)^{p_3}\frac{\ln(u)}{u} \times 10^{-18}\ {\rm cm}^2, \quad (1)$$

where $u = E/E_{\rm th}$ is the incident electron energy E, in eV, normalized by the direct multiple-ionization threshold $E_{\rm th}$ and $E_{\rm Ryd} = 13.606$ eV. The parameters p_0 and p_2 depend on the number of electrons being removed and have been tabulated by Shevelko & Tawara (1995b) and Bélenger et al. (1997). The parameter p_1 is the number of electrons in the target ion, and $p_3 = 1.0$ for neutral targets or 0.75 for ionic targets. Shevelko & Tawara (1995a, 1995b) and Bélenger et al. (1997) obtained these fitting parameters by comparing with relatively heavy targets, such as Kr^{0+}, Xe^{0+}, and Rb^{1+}. For lighter systems, we found that this formula often overestimates the cross section, and so we introduced an additional scaling factor f in order to obtain a better fit to the experimental data. An advantage of this formula is that it can represent the ejection of between two and ten electrons, whereas other formulae are best suited only for double ionization.

The direct double ionization of light ions is often more accurately described by Shevelko et al. (2005),

$$\sigma_{\rm D} = [1 - {\rm e}^{-3(u-1)}]\left\{\frac{p_0}{E_{\rm th}^3}\left[\frac{u-1}{(u+0.5)^2}\right]\right\} \times 10^{-13}\ {\rm cm}^2. \quad (2)$$

Here, $E_{\rm th}$ is the threshold for direct EIMI, and p_0 and p_1 are fitting parameters. Shevelko et al. (2005) give parameters for p_0 that vary depending on the initial isoelectronic sequence and are valid for He-like through Ne-like ions as well as for Ar^{0+}–Ar^{7+}. As described below, we found that, with a few slight adjustments, their argon fitting parameters also describe reasonably well the rest of the ions in the corresponding isoelectronic sequences. For near-neutrals, we found that the p_0 values given by Shevelko et al. (2005) systematically underestimate the direct double-ionization cross sections, and we provide new p_0 values for cases where there are sufficient data, a point that will be further illustrated in Section 3.

Shevelko et al. (2005) also gave a semiempirical formula for IA causing double ionization of light ions,

$$\sigma_{\rm IA} = f_{\rm BR}\frac{p_0}{E_{\rm th}^2}\frac{u-1}{u(u+p_1)} \times 10^{-13}\ {\rm cm}^2, \quad (3)$$

where $E_{\rm th}$ is the IA threshold, i.e., the threshold for single ionization of a core electron forming an intermediate state that can autoionize. The parameters p_0 and p_1 depend on the isoelectronic sequence of the initial ion configuration. Here, we introduce the quantity $f_{\rm BR}$, which is the branching ratio for autoionization of the intermediate state that is missing an inner-shell electron.

We generally take the IA branching ratios from Kaastra & Mewe (1993), although other calculations of branching ratios exist (e.g., Bautista et al. 2003; Gorczyca et al. 2003, 2006; Palmeri et al. 2003, 2011, 2012; Mendoza et al. 2004; Hasoğlu et al. 2006; Garcia et al. 2009; Kučas et al. 2015). Gorczyca et al. (2003) found that their branching ratios are roughly in agreement with those of Kaastra & Mewe (1993) for light ions, $Z \lesssim 20$, but there are significant discrepancies for heavier ones. An improved set of branching ratio data would be very useful, but for now, the set in Kaastra & Mewe (1993) remains the only comprehensive data set. In Section 3, we point out some specific instances where we find discrepancies that can be attributed to inaccurate branching ratios.

Shevelko et al. (2006) also presented experimental fits to double-ionization data for a few ions. These fits are more accurate than the general formula above. In this scheme, the direct cross section is given by

$$\sigma_{\rm D} = 1 - e^{-3(u-1)}\frac{p_0}{E_{\rm th}^3}\left[\frac{u-1}{(u+0.5)^2}\right][1 + 0.1\ln(4u+1)] \times 10^{-13}\ {\rm cm}^2, \quad (4)$$

where p_0 is a fit parameter. The IA cross sections are given by

$$\sigma_{\rm IA} = \frac{p_0}{E_{\rm th}^2}\frac{u-1}{u(u+5.0)}\left[1+\frac{0.3}{p_1}\ln(4u+1)\right]\times 10^{-13}\,{\rm cm}^2, \quad (5)$$

where p_0 is a fit parameter and p_1 is the principal quantum number of the core electron that is directly ionized. Unlike for Equations (2) and (3), the parameters for Equations (4) and (5) do not depend on the isoelectronic sequence, but instead are set by fits to specific experiments. As a result, these formulae are not suitable for extension to unmeasured systems.

In many cases, the IA process can be represented very well by the Lotz formula (Lotz 1969) for single ionization of a core electron multiplied by the branching ratio $f_{\rm BR}$ for autoionization of the resulting intermediate state,

$$\sigma_{\rm IA} = 4.5 f_{\rm BR} p_0 \frac{\ln(u)}{E_{\rm th}^2 u}\times 10^{-14}\,{\rm cm}^2. \quad (6)$$

Here, p_0 is the initial number of electrons in the subshell where ionization takes place and $E_{\rm th}$ is the threshold for single ionization of that subshell. The needed branching ratios for many ions of astrophysical interest have been given by Kaastra & Mewe (1993). As mentioned above, updated calculations for some systems have been reported. However, in most cases, those calculations are less useful for estimating EIMI cross sections, because they report a total radiative yield but do not give a breakdown of the branching ratios for each number of electrons ejected.

Several other formulae have been proposed for representing EIMI cross sections. Fisher et al. (1995) gave a set of two formulae that are relevant at low and high energies. As it is a somewhat more complicated scheme than any of the above formulae and the data can be adequately represented using a simpler approach, we opted not to use the Fisher et al. formulae. Talukder et al. (2009) also describe an approach for fitting double-ionization cross sections for some light and low-charge ions, but their parameters are direct fits to experimental data and so cannot be directly extended along isoelectronic sequences.

3. Fitting Formulae and Parameters by Isoelectronic Sequence

We fit the above cross-section formulae to various reported EIMI measurements. Table 1 gives the bibliographic references for the experimental EIMI data, organized by isoelectronic sequence and order of EIMI (i.e., double, triple, quadruple, etc.). Although all of the above formulae have been developed for or previously applied to some experimental data, our purpose in doing this new comparison was to determine the following: first, whether the formulae remained valid in light of data that have been published more recently. Second, under which conditions, such as isoelectronic sequence and nuclear charge Z, each semiempirical formula best represents the data. And third, to revise the parameters when necessary for our applications. In this section, we report the results by isoelectronic sequence.

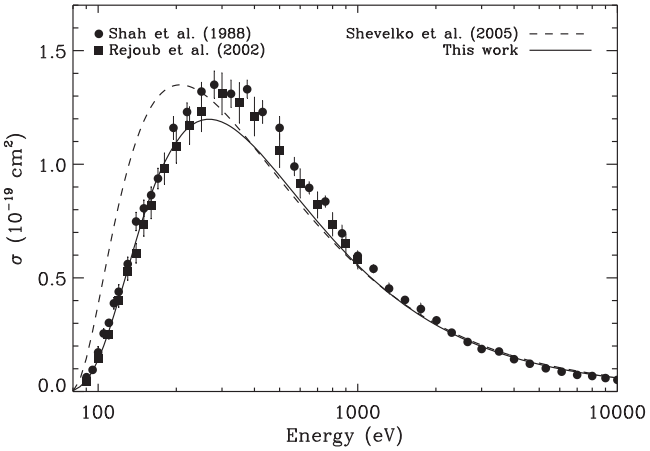

Figure 1. Double ionization of He^{0+} forming He^{2+}. The data points show the experimental results of Shah et al. (1988; filled circles) and Rejoub et al. (2002; filled squares). The dashed line illustrates the semiempirical formula following Shevelko et al. (2005), and the solid line uses the cross-section scaling found here for He-like systems.

In the following, the direct EIMI thresholds are from Kramida et al. (2016) and represent the sum of the single-ionization thresholds from the initial charge state q_i to the final charge state q_f. The IA thresholds are the single-ionization thresholds for the core electrons and are taken from Kaastra & Mewe (1993), except for some light ions and the low-charge ions of argon, for which more recent data are given in Shevelko et al. (2005). We also do not account for relativistic effects, which may be relevant as collision energies become significant compared to the electron rest mass. For single ionization, relativistic corrections become noticeable at about 20 keV (Kim et al. 2000).

Table 2 presents a sample of the machine-readable table, which lists the parameters used for each cross section. In that table, each ion is denoted by the nuclear charge Z, initial charge state q_i, and final charge state q_f. The total cross section is the sum of all individual cross sections having the same set of Z, q_i, and q_f. Also, although we previously reported EIMI cross-section estimates for Fe (Hahn & Savin 2015a), here we made some minor revisions to those cross sections based on the current analysis of a wider range of ions.

3.1. He-like

He-like ions are difficult to fit using any of the semiempirical formulae described above. The dashed curve in Figure 1 illustrates the formula using Equation (2) from Shevelko et al. (2005) compared to various double-ionization measurements of neutral He (Shah et al. 1988; Rejoub et al. 2002). There is clearly an offset in the energy position of the peak cross section. Similar results are found for other He-like ions.

In order to fit the He-like data, we compared double-ionization cross-section data for H^- (Yu et al. 1992), He^{0+} (Shah et al. 1988; Rejoub et al. 2002), and Li^{1+} (Peart & Dolder 1969). Figure 2 shows that if the cross-sections are scaled by a factor of $E_{\rm th}^{-2.6}$ and plotted against the normalized energy $E/E_{\rm th}$, then the scaled cross sections agree very well (see also Müller 2005). Kim & Rudd (1994) suggested that double ionization of He-like ions should be well fit by a

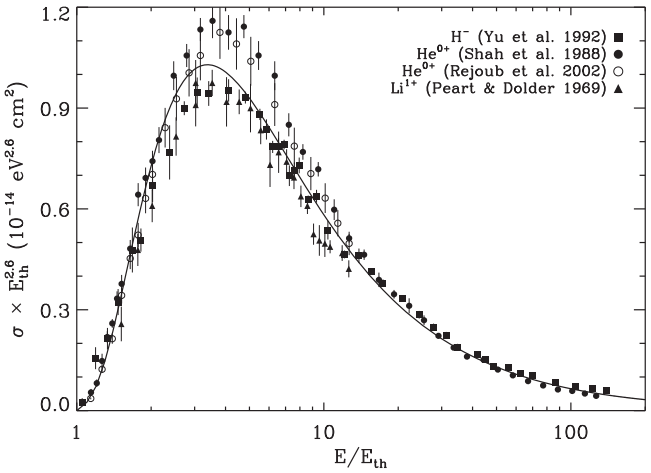

Figure 2. Scaled double-ionization cross sections for the He-like systems H^-, He^{0+}, and Li^{1+}. The solid line shows our fit to the scaled data using Equation (7).

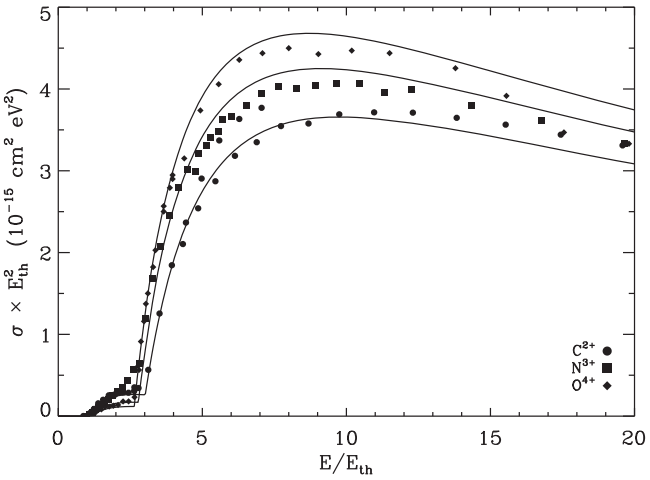

Figure 3. Scaled double-ionization cross sections for several Be-like ions: C^{2+}, N^{3+}, and O^{4+}. The symbols show the measurements of Westermann et al. (1999), and the solid curves are the cross sections reported here, which in this case use the semiempirical scheme of Shevelko et al. (2005).

function of the form:

$$\sigma = \frac{1}{E_{\rm th}^{p_0}}\frac{1}{u}\left[p_1\left(1-\frac{1}{u}\right)+p_2\frac{\ln(u)}{u}+p_3\frac{\ln(u)}{u^2}+p_4\frac{\ln(u)}{u^3}\right] \times 10^{-14}\ \mathrm{cm}^2. \quad (7)$$

Here, $p_0 = 2.6$ is the scaling factor described above. The parameters p_1–p_4 are determined from the fit to the scaled data and are given in Table 2. This function fits the scaled data very well as shown by Figure 2. The solid curve in Figure 1 shows our results applied to the double ionization of He^{0+}.

We extrapolate the He-like double-ionization cross sections to unmeasured systems using Equation (7). Note that all of the parameters p_0–p_4 are the same within the isoelectronic sequence, with the only change coming from varying $E_{\rm th}$. Measurements of double ionization for heavier He-like ions would be useful in order to assess the accuracy of this extrapolation.

For other isoelectronic sequences, the peak of the direct double-ionization cross section occurs roughly in the position predicted by Equation (2). That is, the formula as presented by Shevelko et al. (2005) is adequate. The reason for the shift of the peak to higher energies for the He-like ions may be due to the strong interaction of the electrons with one another for these two-electron systems (Defrance et al. 2000, 2003; Shevelko et al. 2005). Experimental measurements of the differential cross section for double ionization of helium also suggest that the dominant DI mechanism is TS2, in which the incident electron collides sequentially with both bound electrons (Lahmam-Bennani et al. 2010).

3.2. Li-like

Double ionization of Li-like ions is described well using Equation (2). For double ionization of Li ($Z = 3$), we found that $p_0 = 5.8$ reproduces well the measured cross sections of Jalin et al. (1973) and Huang et al. (2002). However, the value $p_0 = 12$ given by Shevelko et al. (2005) matches the measured cross sections for C^{3+} and N^{4+} of Westermann et al. (1999) very well. Lacking any additional experimental data, for all cross sections with $Z \geqslant 4$, we set $p_0 = 12$. IA does not contribute because the resulting excited state lies below the ionization threshold. That is, a vacancy in the K-shell is filled by the relaxation of the $2s$ electron. As there is no other electron in an outer shell that can absorb the energy, only radiative relaxation is possible.

The only Li-like system for which triple-ionization data are available is Li, for which Huang et al. (2003) measured the ratio of triple to double ionization at 1000 eV to be about 1×10^{-3}. To match the cross section implied by this ratio, we rescaled Equation (1) by $f = 0.003$, while otherwise using the triple-ionization parameters given by Shevelko & Tawara (1995b). This is a very large discrepancy for the unaltered prediction formula and is possibly due to the formula having been developed on the basis of data for ions with many more electrons. We ignore triple ionization of Li-like ions for higher-Z ions, because the cross section for Li is already very small and is expected to decrease strongly with increasing Z. Data are lacking for other ions.

3.3. Be-like

For this sequence, double-ionization measurements exist for B^{1+}, C^{2+}, N^{3+}, O^{4+}, and Ne^{6+}. All of these appear to be well-matched by summing Equations (2) and (3) with the parameters for direct double ionization given by Shevelko et al. (2005). Examples of these fits for C^{2+}, N^{3+}, and O^{4+} are shown in Figure 3 and compared to the data of Westermann et al. (1999). For the figure, the cross-section data have been scaled by a factor of $E_{\rm th}^2$. As the charge state increases, IA becomes increasingly important relative to DI. Kaastra & Mewe (1993) give the branching ratio for IA of Be-like ions as unity; however, the calculations of Shevelko et al. (2005) suggest that for high-Z ions, the branching ratio is closer to 90%. We are not aware of any experimental data for systems above $Z = 10$ that we could compare to, but this would be a relatively modest error. On the basis of these data, we infer the cross sections for all other Be-like ions using Equations (2) and (3) with branching ratios from Kaastra & Mewe (1993).

Theoretical calculations were performed for double ionization of both Be^{0+} and B^{1+} using time-dependent close-coupling R-matrix and distorted-wave methods (Pindzola et al. 2010, 2011). Their calculations for B^{1+} are in good

agreement with experimental data. However, for Be^{0+}, there are no experimental data with which to compare. The semiempirical prediction for DI of Be^{0+} is about 50% larger than predicted by theory, but the larger IA contributions appear to be roughly in agreement. Given that the theory is accurate for B^{1+} and that the semiempirical formula seems to overestimate the direct double-ionization cross section for very low-charge states in nearby isoelectronic sequences (e.g., Li-like and B-like), it is possible that the Be^{0+} theory is correct and that the semiempirical formula is an overestimate here as well. Experimental measurements would be beneficial to resolve this discrepancy, but for now we use the semiempirical prediction.

Because the state resulting from a K-shell vacancy lies below the double-ionization threshold for the resulting system, net triple and quadruple ionization of Be-like ions can only proceed via DI processes. As there are no measurements and we expect these cross sections to be very small, as they are for the triple ionization of Li (Section 3.2), we ignore them.

3.4. B-like

Double ionization of B-like ions is generally well-described using Equations (2) and (3). For DI using Equation (2), Shevelko et al. (2005) recommend $p_0 = 10$, which matches the experiments for N^{2+}, O^{3+}, and Ne^{5+}, but not the data for C^{1+}. For C^{1+}, we set $p_0 = 8.24$ to match the cross-section data of Westermann et al. (1999). For DI of all other ions, we set $p_0 = 10$. Based on our results for other near-neutral species, this may overestimate the DI cross section for B^{0+}.

IA contributes to the double ionization of B-like ions and may also contribute to their triple ionization. The predicted IA branching ratios for B-like ions can be benchmarked by comparing to the experiments. Kaastra & Mewe (1993) write that following the ionization of a 1*s* electron, the B-like ions either radiatively stabilize for a net single ionization or eject one electron leading to a net double ionization. They predict that the branching ratio for triple ionization is zero. However, measurements of triple ionization for C^{1+}, N^{2+}, and O^{3+} by Westermann et al. (1999) suggest that IA does contribute to triple ionization. These cross sections can be well-described by the Lotz cross-section, i.e., Equation (6), for single ionization of the 1*s* electron multiplied by a factor of 0.068, 0.04, or 0.024, respectively. This suggests that the branching ratio for triple ionization has a magnitude of a few percent.

Another indication that IA leads to triple ionization comes from the double-ionization measurements of Ne^{5+} by Duponchelle et al. (1997). These double-ionization data could be better fit by Equation (3) if the IA branching ratio were reduced by 0.1 from the Kaastra & Mewe prediction of 0.98 to about 0.88. The reduction suggests that Ne^{5+} could have an IA branching ratio for triple ionization of up to ~0.1.

Triple ionization of B-like C, N, and O are best described as being due solely to IA using the Lotz formula multiplied by the empirical branching ratios given above. We use the same method to estimate the cross section for triple ionization of Ne^{5+}, although, as discussed above, the estimate for that ion is not based directly on triple-ionization measurements but rather inferred from the double-ionization cross section. For other B-like ions, we assume that IA will continue to dominate the cross section and adopt an estimated branching ratio of $f_{BR} = 0.06$, which is the average of the branching ratios we estimated above based on the C, N, O, and Ne data. For consistency, we also reduce the corresponding branching ratios for double ionization by 0.06 to account for the fraction that we now ascribe to triple ionization.

We ignore quadruple- and higher-order EIMI processes, as we are unaware of any measurements beyond triple ionization, and such cross sections are likely to be very small as they would require breaking open the K-shell.

3.5. C-like

Double and triple ionization of C-like ions are estimated in a similar way as for B-like ions. For double ionization, Shevelko et al. (2005) sets $p_0 = 23$ in Equation (2). This is accurate compared to measurements of O^{2+} and Ne^{4+}, but we reduce p_0 to 19.2 in order to match the double-ionization measurements of N^{1+} by Lecointre et al. (2013). Nitrogen measurements were also reported by Zambra et al. (1994), but their cross section is about 30% smaller than that of Lecointre et al. (2013). We chose not to rely on the Zambra et al. (1994) results, because they appear to be systematically smaller than the results of other groups. Triple-ionization measurements for N and O suggest that the IA branching ratio for triple ionization is about 0.07 and 0.075, respectively, and so we reduce the Kaastra & Mewe (1993) IA branching ratio for double ionization by these amounts in order to account for the fraction of IA that leads to triple rather than double ionization.

The triple-ionization measurements for N and O are best modeled as dominated by IA using the Lotz formula. Based on these results, we estimate the cross section for other C-like ions in the same way, adopting a branching ratio of $f_{BR} = 0.07$. Consistent with this representation for triple ionization, we reduce the branching ratios for double ionization by 0.07 from the Kaastra & Mewe (1993) values.

Quadruple ionization of N^{1+} was measured by Lecointre et al. (2013). None of the formulae seem to match the data very well, but the data are also not very detailed with large statistical error bars. Assuming that the cross section is due to 1*s* IA using Equation (6), a branching ratio for quadruple ionization of 1.4×10^{-3} would approximate the magnitude of the cross section, but the energy threshold is too low. An alternative is the indirect MIMA process in which direct double ionization of a 1*s* and a 2*s* electron leads to a system that subsequently relaxes through double autoionization, giving a net quadruple ionization. Using the Los Alamos Atomic Physics Code (Magee et al. 1995), we estimate that the threshold for this process is about 496 eV, which would match the apparent threshold in the data quite well. Based on this, we model the cross section as direct double ionization of a 1*s* and 2*s* electron pair using Equation (1) for double ionization with a threshold of ≈496 eV and scaled by a factor of $f = 0.0225$ to match the data. This f could be interpreted as the branching ratio for quadruple ionization after forming the two "holes" in the 1*s* and 2*s* subshells. However, given that Equation (1) can sometimes be very inaccurate for predicting double ionization, the inferred branching ratio should be regarded as an order of magnitude estimate, at best.

To estimating quadruple ionization of other C-like ions, we scale Equation (1) by a factor of $f = 0.1$. This scaling is based on considering what is needed to match the magnitude of the quadruple-ionization cross sections for C-, N-, and Ne-like

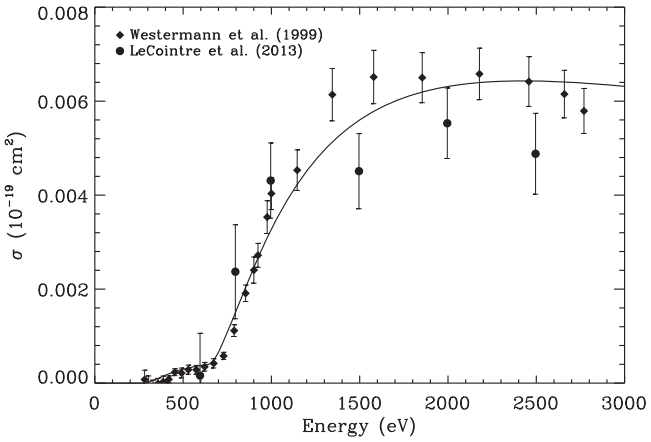

Figure 4. Quadruple ionization of O^{1+} forming O^{5+}. The filled diamonds show the measurements of Westermann et al. (1999), and the filled circles indicate those of Lecointre et al. (2013). The solid curve is our model of the data, as described in Section 3.6.

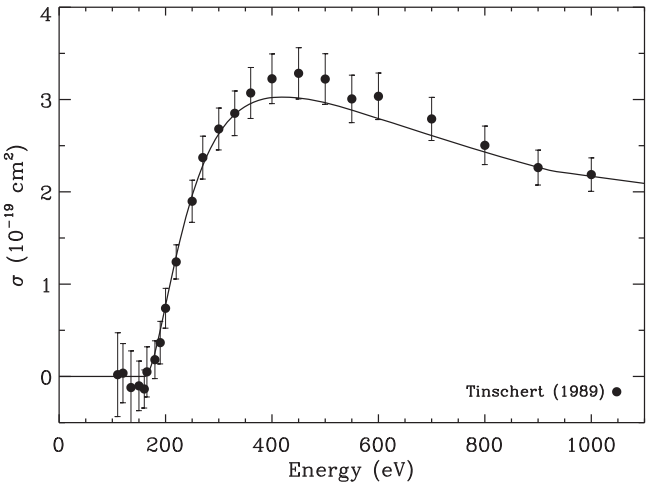

Figure 5. Double ionization of Ne^{2+} forming Ne^{4+}. The symbols show the measurements of Tinschert (1989), and the solid curve is our fit to the data as described in Section 3.7.

ions. For example, scaling Equation (1) by a factor of $f \approx 0.04$ would roughly match the peak of the quadruple-ionization cross section for N^{1+}, while factors of $f \approx 0.06$ and $f \approx 0.12$ would suffice for quadruple ionization of N-like O^{1+} and Ne-like Ne^{0+}, respectively. We apply this approach to estimate the quadruple-ionization cross section for all ions that lack experimental data in the C-like through Ne-like isoelectronic sequences. This approximation probably underestimates the effective energy threshold for quadruple ionization, because the thresholds for the important indirect processes lie at higher energies than the DI threshold used in Equation (1). EIMI beyond quadruple ionization is ignored for C-like ions.

3.6. N-like

Double ionization of the N-like ions O^{1+}, Ne^{3+}, and Ar^{11+} is well-described by Equations (2) and (3) using the parameters given by Shevelko et al. (2005) and the branching ratios for IA from Kaastra & Mewe (1993). We apply the same scheme to double ionization of all other N-like ions.

Triple- and quadruple-ionization measurements exist for O^{1+} (Westermann et al. 1999; Lecointre et al. 2013). For triple ionization, the data can be best modeled by scaling Equation (1) by a factor of $f = 0.056$ with the other parameters given by Shevelko & Tawara (1995b) and adding to that an IA contribution modeled using Equation (6) for the K-shell ionization with a branching ratio of $f_{BR} = 0.108$. This inferred triple-ionization branching ratio is roughly similar to that found in photoionization measurements of N^{0+} by Stolte et al. (2016). The direct and indirect contributions to triple ionization are of similar magnitude. For triple ionization of other N-like ions, we scale Equation (1) by a factor of $f = 0.15$, which has the observed threshold for direct triple ionization and roughly matches the magnitude of the total cross section for N-like ions, as well as for nearby isoelectronic sequences. There is not sufficient data to reliably separate the DI and IA contributions.

Figure 4 shows the quadruple-ionization cross section for O^{1+}. Similar to N^{1+}, this can be modeled as the sum of direct quadruple ionization, plus an indirect cross section due to MIMA, where direct double ionization of both a 1*s* and 2*s* electron results in a system that relaxes through further double autoionization. The data show that the cross section begins to rise at the direct quadruple-ionization threshold of about 281 eV and that this appears to be the only contribution to the cross section until ~650 eV. This direct cross section is well-matched by Equation (1) scaled by $f = 0.005$. In principle, we might expect IA from the K-shell to lead to quadruple ionization, but no increase in the cross section is seen until about 100 eV above the K-shell ionization threshold of ≈568 eV. Using the Los Alamos Atomic Physics Code (Magee et al. 1995), we estimate that the threshold for direct double ionization of a 1*s* and 2*s* electron pair is ≈646 eV, which matches the threshold in the data. We estimate the MIMA cross section using Equation (1) for the double ionization of the 1*s* and 2*s* electron pair scaled by a factor of $f = 0.078$. This scaling factor can be thought of as the branching ratio for the system to relax by double autoionization. However, it is better to consider it a fitting parameter only, because for it to be a quantitative estimate of the branching ratio requires that Equation (1) accurately estimate the inner-shell direct double-ionization cross section, which may not be the case.

Although MIMA appears to dominate the O^{1+} quadruple-ionization cross section, there are not sufficient data to extrapolate its contribution to the other N-like systems. Instead, we estimate quadruple ionization for the other N-like ions using Equation (1) scaled down by a factor of $f = 0.1$, as described above in Section (3.5).

3.7. O-like

Equations (2) and (3), with parameters from Shevelko et al. (2005) and IA branching ratios from Kaastra & Mewe (1993), match well the experimental measurements of double ionization of the O-like ions F^{1+}, Ne^{2+} (Figure 5), and Ar^{10+} (Figure 6). However, the same procedure overestimates the cross section for O^{0+} by about a factor of two. To correct for that, we set $p_0 = 39$ in Equation (2) for double ionization of neutral oxygen. For all other ions, we make no modifications.

We are not aware of any triple- or higher-order EIMI measurements for these ions. On the basis of results for nearby isoelectronic sequences, we model triple and quadruple ionization using Equation (1) scaled by a factor of $f = 0.15$ and $f = 0.1$, respectively.

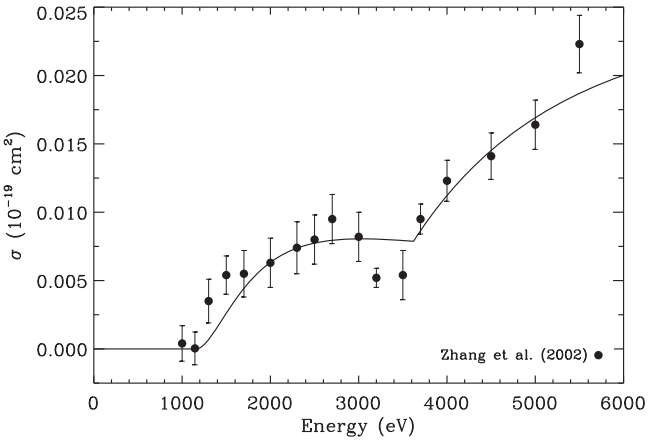

Figure 6. Double ionization of Ar^{10+} forming Ar^{12+}. The symbols show the measurements of Zhang et al. (2002), and the solid curve is our fit to the data as described in Section 3.7.

3.8. F-like

Double-ionization measurements exist for Ne^{1+} (Tinschert 1989; Zambra et al. 1994), Al^{4+} (Steidl et al. 1999), and Ar^{9+} (Zhang et al. 2002). We find that Equations (2) and (3) can match the measured cross sections well. However, for neon, we must set $p_0 = 76.7$ in Equation (2) to match the data, which is significantly smaller than the recommended value of $p_0 = 133$ (Shevelko et al. 2005). The unmodified parameters do describe the aluminum and argon data well.

Figure 7 shows the triple-ionization cross section for Ne^{1+} forming Ne^{4+}, which was measured by Tinschert, Müller, Hofmann, and Salzborn (Tinschert 1989, unpublished). There is also a separate unpublished measurement from the same group. Generally, we fit triple-ionization cross sections using Equation (1) for DI and model the IA using the Lotz cross section. However, for Ne^{1+}, the peak of the cross section is narrower than implied by Equation (1), so we use Equation (2) instead and set $p_0 = 12$ to match the experiment. An inflection is visible in the cross section at about 1000 eV, suggesting an indirect ionization process, but the indirect contribution is relatively small and so we ignore it for this ion.

For triple ionization of F-like ions other than Ne^{1+} and quadruple ionization of all F-like ions, we use the same interpolation procedure as for other nearby isoelectronic sequences: Equation (1) multiplied by factors of $f = 0.15$ for triple ionization and $f = 0.1$ for quadruple ionization. If we were to use this scheme to estimate the Ne^{1+} triple-ionization data, we would find that it is somewhat inaccurate as it overestimates the cross section at higher energy. Unfortunately, there are not enough data to test an alternative model.

3.9. Ne-like

There are several measurements for EIMI of neutral Ne^{0+} forming Ne^{2+}–Ne^{5+} (see Table 1). Equation (2) can accurately match the double-ionization measurements for Ne^{0+} if $p_0 = 48.4$, which is significantly smaller than the recommended value of $p_0 = 183$ (Shevelko et al. 2005).

IA is also expected to contribute to double ionization and can be included via Equation (3). Kaastra & Mewe (1993) give a branching ratio of $f_{BR} \approx 0.98$ for the net double ionization of Ne^{0+}, and they predict no contribution to triple or higher EIMI due to IA. Müller et al. (2017) recently studied photoionization

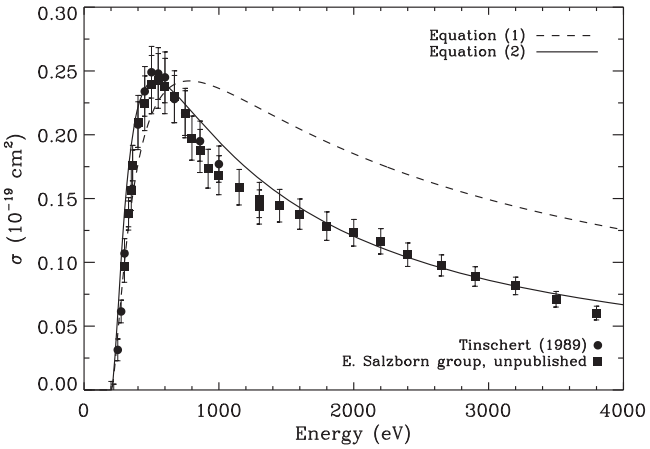

Figure 7. Triple ionization of Ne^{1+} forming Ne^{4+}. The filled circles show the data of Tinschert (1989) and the filled squares indicate other unpublished data from the group of E. Salzborn (2016, private communication). The dashed curve uses Equation (1), but the peak is clearly broader than the measurement. Instead, we fit the data using Equation (2). Although developed for double-ionization cross sections, it fits these triple-ionization data well.

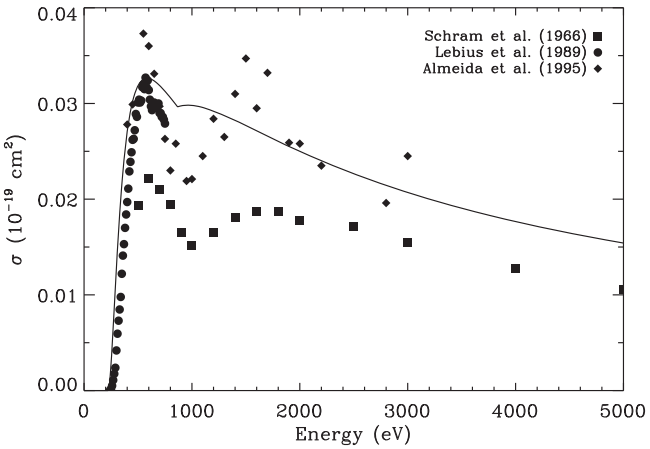

Figure 8. Quadruple ionization of Ne^{0+} forming Ne^{4+}. The filled squares show the measurements of Schram et al. (1966), the filled circles those of Lebius et al. (1989), and the filled diamonds those of Almeida et al. (1995). The solid curve is our model of the data as described in Section 3.9.

of Ne atoms and Ne^{1+} ions, and measured the K-shell branching ratio to be $f_{BR} = 0.93$ for double ionization of Ne^{0+}, and we use this value to calculate the cross section, $f_{BR} \approx 0.76$.

Direct triple ionization of neon is also well fit using Equation (2) with $p_0 = 16.6$, where again we used this semiempirical formula that is normally intended for double ionization because it matches the sharper measured peak better than Equation (1). The IA contribution is represented using Equation (3). Müller et al. (2017) found a branching ratio of $f_{BR} = 0.054$, which fits these data reasonably well. As usual, we are assuming that the only relevant indirect process is the single ionization of a $1s$ electron with subsequent Auger decays.

The contribution of indirect processes is clear in the Ne^{0+} quadruple- and quintuple-ionization cross sections, shown in Figures 8 and 9, respectively. There, the measurements imply branching ratios of ≈0.02 for quadruple ionization and ≈0.004 for quintuple ionization. This quadruple-ionization branching ratio is an order of magnitude larger than that measured due to photoionization by Müller et al. (2017), who found

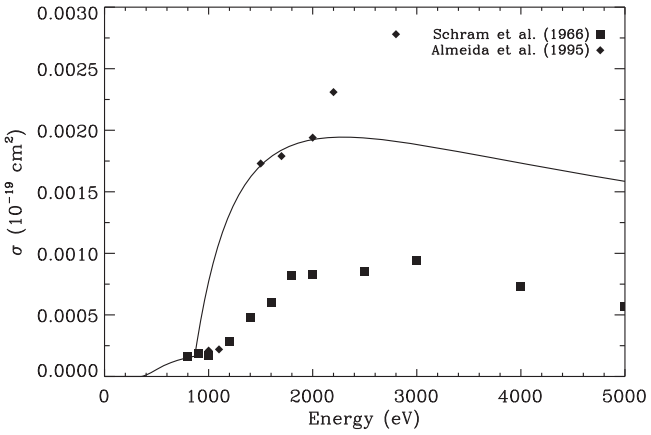

Figure 9. Quintuple ionization of Ne^{0+} forming Ne^{5+}. The filled squares show the measurements of Schram et al. (1966) and the filled diamonds those of Almeida et al. (1995). The solid curve is our model of the data as described in Section 3.9.

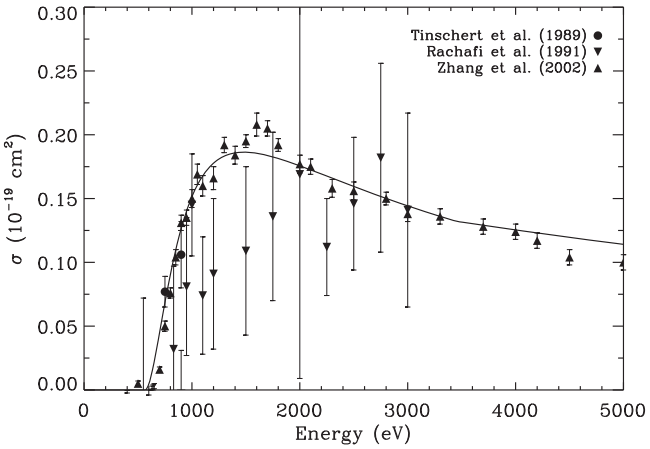

Figure 10. Double ionization of Ar^{7+} forming Ar^{9+}. The filled circles show the data of Tinschert et al. (1989), the upward-pointing triangles the data of Rachafi et al. (1991), and the downward-pointing triangles the data of Zhang et al. (2002). The solid curve illustrates our fit of the data using Equations (2) and (3).

$f_{BR} = 0.002$. The discrepancy is possibly due to the contribution to the EIMI cross section of other indirect ionization processes, such as MIMA. We should also note that for quintuple ionization, there is a very large discrepancy of more than a factor of two between the measurements of Schram et al. (1966) and Almeida et al. (1995). The Schram et al. (1966) results appear to be systematically low for all of the neon EIMI data (compare Figures 8 and 9), so we base the branching ratio above on the Almeida et al. (1995) measurements. We describe the direct quadruple-ionization cross section using Equation (2) with $p_0 \approx 2.2$ and the direct quintuple ionization is modeled with Equation (1) scaled by a factor of $f = 0.005$ to match the cross section below the IA threshold.

Returning to double ionization of other Ne-like ions, measurements exist for Na^{1+}, Al^{3+}, and Ar^{10+}. We fit all of these data using Equation (2) for the DI and Equation (3) for the indirect contribution. For the direct contribution, we find that p_0 often differs from the recommended value from Shevelko et al. (2005) of $p_0 = 183$, with $p_0 = 91.5$ for Na^{1+}, 183 for Al^{3+}, and 201.6 for Ar^{10+}. The discrepancy is largest for low-charge states and matches the nominal value for higher-charge states. This is consistent with what we have seen for other isoelectronic sequences. Based on these measurements, we estimate the double ionization of the unmeasured Ne-like ions using the same equations with the unmodified p_0 value from Shevelko et al. (2005) for Equation (2) and the IA branching ratios from Kaastra & Mewe (1993) in Equation (3).

We estimate the cross sections for the triple and quadruple ionization of $Z \geqslant 11$ Ne-like ions using Equation (1). Scaling factors of $f = 0.4$ and $f = 0.12$ provide a reasonable match to the magnitude of the Ne^{0+} triple- and quadruple-ionization cross sections, respectively. Triple ionization of Al^{3+} is well-described by Equation (1) with $f = 0.13$. Based on these results and on the data for nearby isoelectronic sequences, we set $f = 0.15$ and $f = 0.1$ for triple and quadruple ionization of Ne-like ions. We ignore quintuple ionization for other Ne-like ions because there is not enough data to justify an extrapolation and because the cross section is very small.

3.10. Na-like

Double-ionization measurements exist for Al^{2+} (Steidl et al. 1999) and for Ar^{7+} (Tinschert et al. 1989; Rachafi et al. 1991; Zhang et al. 2002). The Ar^{7+} measurements are illustrated in Figure 10. For Ar^{7+}, the DI contribution can be matched well using Equation (2), setting $p_0 \approx 204.7$. This is a factor of 10 smaller than the value of $p_0 = 2000$ recommended by Shevelko et al. (2005). However, they also based their parameters on the argon data, so we believe this is simply a typographical error in that work. The same formula with $p_0 = 200$ also matches the Al^{2+} double-ionization data well near the ionization threshold, although it underestimates the cross section at the peak and higher energies by about 30%. Based on these results, we estimate the direct double ionization of other Na-like ions by setting $p_0 = 200$. For the indirect ionization of Na-like ions, including Ar^{7+}, we use Equation (3) with the branching ratio from Kaastra & Mewe (1993). There is also a double-ionization measurement of Na^{0+} by Tate & Smith (1934), which we approximate well using Equation (1) with $f = 1$ and incorporating IA via Equation (6) with the Kaastra & Mewe (1993) branching ratios. As with other very low-charge states, Equation (2) can only match the Na^{0+} cross section if one uses a much smaller value of p_0, here $p_0 \sim 10$.

Triple ionization of Al^{2+} forming Al^{5+} was measured by Steidl et al. (1999). These data can be well-described by Equation (1) with $f = 0.27$ from the triple-ionization threshold of ≈300 eV up to the peak of the cross-section at ≈1000 eV. However, the peak from the semiempirical formula is broader than that of the experimental result, resulting in a discrepancy of a factor of two at very high energies ∼5000 eV. An alternative fitting scheme is to use Equation (2) with $p_0 = 28.6$, which matches the high-energy data well, but rises too fast above the threshold. Because we expect the low-energy data to be the most important for typical applications, we used the fit based on Equation (1).

Considering our results for Al^{2+} and for other isoelectronic sequences between Na-like through Ar-like ions, we estimate the triple- and quadruple-ionization cross section with Equation (1), setting $f = 0.2$ and $f = 1$, respectively. For quadruple ionization, this approximation, which is based on the DI energy threshold, probably underestimates the effective energy threshold due to the importance of indirect processes that turn on at higher energies. Quintuple and higher EIMI are neglected.

3.11. Mg-like

We estimate the double-ionization cross sections of Mg-like ions using Equation (2) with $p_0 = 1$ and Equation (3). In order to match the double-ionization measurements of Mg^{0+} (McCallion et al. 1992b; Boivin & Srivastava 1998) and Al^{1+} (Steidl et al. 1999), we need to increase p_0 in Equation (2) to 1.46 and 2.24, respectively, from the recommended value of 1 (Shevelko et al. 2005). However, these are small corrections to the overall cross sections, which are dominated by IA. This IA is probably from the ionization of an $n = 2$ electron, based on the apparent threshold. We model this indirect cross section for Mg-like ions, using Equation (3) and Kaastra & Mewe (1993) branching ratios. This does, however, overestimate both the Mg^{0+} and Al^{1+} cross sections compared to experimental results by up to a factor of two. We found a similar, but smaller, discrepancy of about 30% between the predicted double-ionization cross section and the measurements for Ar^{6+}.

The reason for these discrepancies is not clear. Since the $n = 2$ single-ionization threshold is below the triple-ionization threshold, an $n = 2$ hole can relax either radiatively leading to a net single ionization or by ejecting a single electron leading to a net double ionization. Considering Mg^{0+}, if we were to ascribe the apparent excess branching ratio to single ionization rather than double ionization, the Mg^{0+} single-ionization cross section would increase by about 20%. Similarly, for Al^{1+}, the increase to the single-ionization cross section would be about 40%. Such large contributions might appear in the single-ionization data as an inflection in the cross section at the $n = 2$ ionization threshold; however, such a features is not apparent in the single-ionization data (Belic et al. 1987; McCallion et al. 1992b; Boivin & Srivastava 1998).

Triple ionization of Mg^{0+} and Al^{1+} can both be fit using Equation (1) with $f = 1$. The fit matches well the data for Mg^{0+} near the threshold, but the peak cross section given by the fit is roughly half of the experimental one. The fit for Al^{1+} rises somewhat faster than the data near the threshold, but the magnitude of the peak cross section is in excellent agreement. For both ions, these discrepancies may be due to additional MIMA processes. Quadruple ionization of Al^{1+} can be described using Equation (1) with $f = 0.27$.

We model triple and quadruple ionization of other Mg-like ions using Equation (1) with $f = 0.2$ for triple ionization and $f = 1$ for quadruple ionization. These values were chosen because they are consistent with the EIMI data for nearby isoelectronic sequences of Na-like through Ar-like ions.

3.12. Al-like

Measurements of the double ionization of Ar^{5+} (Tinschert et al. 1989; Zhang et al. 2002) are well-described by Equations (2) and (3) with the Shevelko et al. (2005) parameters and Kaastra & Mewe (1993) branching ratios, so we use these formulae for Al-like ions up to Ca ($Z \leqslant 20$). There is about a 20% discrepancy with the measurements for Ar^{5+}, which appears to be due to the IA being overestimated when using the branching ratios from Kaastra & Mewe (1993). One way to resolve this discrepancy would be to reduce the $2s$ branching ratio for double ionization from the Kaastra & Mewe (1993) value of $\approx$0.99 to $\approx$0.18, where the excess branching ratio might go toward either single or triple ionization. Alternatively, the $2p$ branching ratio could be reduced, with the excess contributing to single ionization. Triple-ionization measurements for Ar^{5+} would be useful to test this. Since the resolution is ambiguous and the error is fairly modest, we still use the Kaastra & Mewe (1993) branching ratios here.

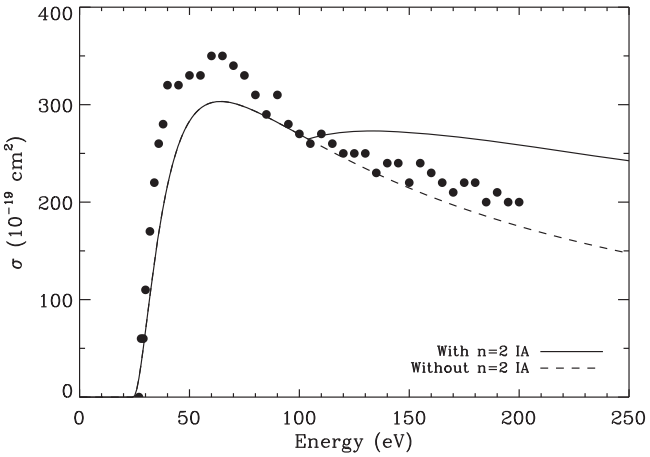

Figure 11. Double ionization of Si^{0+} forming Si^{2+}. The filled circles show the data of Freund et al. (1990). The solid curve shows our estimate using the branching ratios of Kaastra & Mewe (1993). The dashed curve illustrates the cross section of the case when the branching ratios are set to zero. It is clear that the true branching ratio is smaller than predicted.

For double ionization of Fe^{13+}, Equations (2) and (3) become less accurate and tend to underestimate the DI while overestimating the indirect contributions. We also find similar issues with later isoelectronic sequences. Those equations were developed by Shevelko et al. (2005) for application to "light positive ions," so it is not surprising that they become less accurate for higher Z. Thus, for estimating the double ionization of Al-like ions with $Z \geqslant 21$ (above Sc), we use Equation (1) with $f = 1$ and the other parameters from Bélenger et al. (1997) to model the DI cross section and add in IA contributions using Equation (6).

We are not aware of any measurements of triple- or higher-order EIMI for Al-like ions. As mentioned above, we estimate the cross sections for these ions using Equation (1) with $f = 0.2$ for triple ionization and $f = 1$ for quadruple ionization. Again, this may underestimate the effective energy threshold, which is probably due to IA rather than the DI represented by Equation (1).

3.13. Si-like

The cross sections of Si-like systems can be estimated in the same way as those of Al-like ions. For $Z \leqslant 20$, double ionization is described by Equations (2) and (3) with the parameters given by Shevelko et al. (2005) for Ar^{4+} and branching ratios from Kaastra & Mewe (1993). For $Z \geqslant 21$, we use Equation (1) with the parameters from Bélenger et al. (1997) and add IA using the Lotz cross-section, i.e., Equation (6), and the Kaastra & Mewe (1993) branching ratios. As was the case for the Al-like ions, we find that the branching ratios for $2p$ IA given by Kaastra & Mewe (1993) are probably overestimated. Figure 11 illustrates this for Si^{0+}, where the discrepancy with the measurements of Freund et al. (1990) is particularly large. For this ion, the $2s$ IA branching ratio predicted by Kaastra & Mewe (1993) is already negligible, only $f_{BR} \approx 0.03$, and so the discrepancy must be due to the $2p$ branching ratio, which Kaastra & Mewe (1993) predict to be $f_{BR} \approx 1$. The triple- and quadruple-ionization

cross sections are estimated following the same procedure as described for Al-like ions (Section 3.12).

3.14. P-like

The total cross sections for double, triple, and quadruple ionization of P-like ions are estimated following the same procedures as for Si-like ions and using the appropriate parameters from Bélenger et al. (1997), Shevelko et al. (2005), and Kaastra & Mewe (1993) in the corresponding semiempirical formulae. We also now add quintuple ionization. Although there are no quintuple-ionization data for P-like ions, we believe this is a reasonable place to start including quintuple ionization, because this is the first M-shell ion for which removing five electrons does not require breaking open the L-shell. We estimate the quintuple-ionization cross sections based on Cl-like and Ar-like data and use Equation (1) with $f = 0.5$ and the other parameters from Shevelko & Tawara (1995b). We also include IA in the quintuple-ionization cross section via Equation (6) multiplied by the branching ratios whenever they are predicted to be non-zero by Kaastra & Mewe (1993).

3.15. S-like

Double-ionization measurements of S^{0+} (Ziegler et al. 1982a; Freund et al. 1990) and Ar^{2+} (Tinschert et al. 1989) can be be fit using Equations (2) and (3), but the p_0 parameter in Equation (2) needs to be increased from the value $p_0 = 40$ given by Shevelko et al. (2005). For sulfur, there is a discrepancy of about 30% between the data of Ziegler et al. (1982a) and those of Freund et al. (1990). For energies below the IA threshold, the Ziegler et al. data can be fit by setting $p_0 = 60$, while the Freund et al. measurements are consistent with $p_0 = 40$. For Ar^{2+}, the experiments of Tinschert et al. (1989) are best fit with a value of $p_0 \approx 56$. Based on these results, $p_0 \approx 60$ is more consistent with the available data, and so we use this value for estimating the direct double-ionization cross section for other S-like ions that have $Z \leqslant 20$.

For double ionization of $Z \geqslant 21$ ions, we follow the same procedure as for the previous isoelectronic sequences and use Equations (1) and (6). One representative cross section from this group exists, which is a measurement of double ionization for Ti^{6+} by Hartenfeller et al. (1998). For that particular ion, we used the fits given by Shevelko et al. (2006), and Equations (4) and (5). For comparison with the $Z \leqslant 20$ ions, we found that a value of $p_0 = 180$ would be needed in Equation (2) in order to approximately match the magnitude of the DI cross section of $Z \geqslant 21$ ions. This is much larger than the value of $p_0 = 60$ of the low-Z data and illustrates that the Shevelko et al. (2005) formulae are less predictive for heavy ions.

Triple ionization has been measured for S^{0+} (Ziegler et al. 1982a) and Ar^{2+} (Müller & Frodl 1980). Both of these cross sections can be accurately represented using Equations (1) and (6). For S^{0+}, the best fit has $f = 0.29$ in Equation (1) and for Ar^{2+}, $f = 0.18$. The other parameters are given by Shevelko & Tawara (1995b) with IA branching ratio data from Kaastra & Mewe (1993). The S^{0+} cross section is illustrated in Figure 12. Based on these values and those for nearby isoelectronic sequences, we model triple ionization of other S-like ions using $f = 0.2$ in Equation (1), as is done for other Na-like through Zn-like ions.

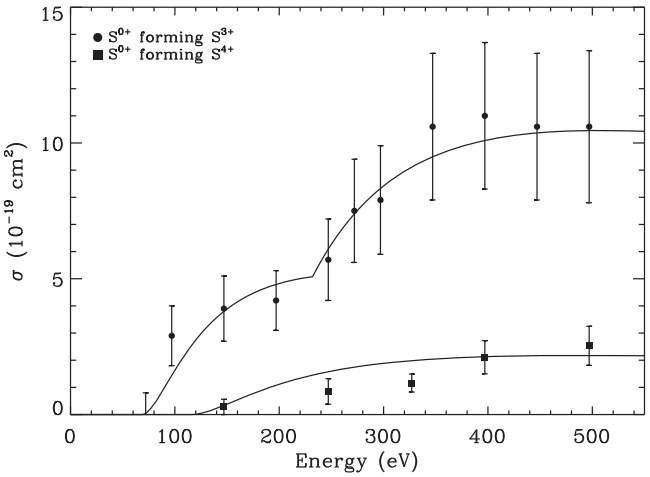

Figure 12. Triple ionization of S^{0+} forming S^{3+} (filled circles) and quadruple ionization of S^{0+} forming S^{4+} (filled squares), from the measurements of Ziegler et al. (1982a). The solid curves show our fits to the data using the semiempirical formulae, as discussed in Section 3.15.

The quadruple ionization of S^{0+} has been measured by Ziegler et al. (1982a) and is well-described by Equation (1) with $f = 1$ (Figure 12). We also include IA using the Lotz cross section and the Kaastra & Mewe (1993) branching ratios, although the relevant IA threshold is at energies much higher than those included in the measurements. We estimate the cross sections for quadruple ionization of other S-like ions using the same scheme as for S^{0+}. Quintuple ionization is included following the procedure described in Section 3.14.

3.16. Cl-like

An extensive set of measurements covering double through septuple ionization of the Cl-like ion Ar^{1+} has been reported by Belic et al. (2010). These data are complemented by the double- and triple-ionization measurements of Müller & Frodl (1980) and Müller et al. (1985). We estimated the empirical branching ratios for IA based on this extensive data set, which gives us an estimate of the possible errors in Kaastra & Mewe (1993) data for L-shell vacancies. Our estimates are limited to the L-shell, because the data do not extend to high enough energies to see the K-shell IA. The IA contributions are most obvious in the higher-order EIMI cross sections. For this reason, we discuss the comparison to the Ar^{1+} data going backwards from septuple ionization. Table 3 summarizes our inferred IA branching ratios for the IA of Ar^{1+} and compares them to the original values from Kaastra & Mewe (1993).

The experimental data for the septuple, sextuple, and quintuple ionization of Ar^{1+} forming Ar^{8+}, Ar^{7+}, and Ar^{6+} all have thresholds that appear to be several hundred electron-volts higher than the DI thresholds. This suggests that the ionization mechanism is dominated by an indirect process. However, the septuple- and sextuple-ionization thresholds are above the single-ionization threshold for an L-shell electron, which indicates the indirect process is not IA from the creation of an L-shell hole. In the case of quintuple ionization, an L-shell vacancy could energetically decay by emitting four additional electrons, but since the experimental data show no cross section until well above the L-shell ionization threshold, the branching ratio for that process must be small. The relevant

Table 3
Inferred IA Branching Ratios for EIMI of Ar^{1+}

Subshell	Source	$\rightarrow Ar^{2+}$	$\rightarrow Ar^{3+}$	$\rightarrow Ar^{4+}$	$\rightarrow Ar^{5+}$	$\rightarrow Ar^{6+}$	$\rightarrow Ar^{7+}$	$\rightarrow Ar^{8+}$
$2p$	This work	0.0004	0.7776	0.222	0	0	0	0
$2p$	Kaastra & Mewe (1993)	0.0004	0.9996	0	0	0	0	0
$2s$	This work	0.0004	0.0348	0.7048	0.26	0	0	0
$2s$	Kaastra & Mewe (1993)	0.0004	0.0348	0.9648	0	0	0	0

indirect process for these EIMI cross sections may be MIMA, where DI of multiple core electrons are followed by the ejection of multiple electrons as the resulting excited state relaxes (see e.g., Section 3.6). For these complex ions, there are several combinations of inner-shell vacancies that could match the apparent threshold, so it is not possible to empirically estimate a model cross section based on MIMA. Instead, we approximately match the magnitude of the measurements using Equation (1) with $f = 0.055$ for septuple ionization, 0.24 for sextuple ionization, and 0.52 for quintuple ionization, though this scheme underestimates the effective threshold energy. In each case, K-shell IA is accounted for via Equation (6) multiplied by the branching ratios from Kaastra & Mewe (1993).

The observed energy threshold for quadruple ionization matches very well with the threshold for single ionization of a $2s$ electron of ≈343 eV (Shevelko et al. 2005). Since the data show no cross section between the DI threshold of ≈203 eV and the $2s$ ionization threshold, the DI and $2p$ IA are negligible. The observed cross section can be fit using the Lotz cross section, i.e., Equation (6), if the branching ratio is $f_{BR} = 0.26$. This is in contrast to Kaastra & Mewe (1993), who predict the branching ratio to be $f_{BR} = 0$. Our empirical estimate assumes that the entire cross section is due to IA from a $2s$ hole, but in reality, other indirect processes may also contribute. Figure 13 compares our cross section to the measurements of Belic et al. (2010).

Figure 13 also illustrates the triple-ionization cross section, which shows evidence that DI can be well-matched by Equation (1) with $f = 0.095$ plus IA added via the Lotz formula multiplied by branching ratios adjusted as follows: the cross section shows a rapid increase below 300 eV, which corresponds well with the $2p$ single-ionization threshold. In order to infer a branching ratio for $2p$ IA, we first reduce the Kaastra & Mewe branching ratio for $2s$ IA leading to triple ionization by 0.26, because we believe that fraction goes to quadruple ionization. This leaves a remaining branching ratio of $f_{BR} = 0.7048$ to go toward $2s$ IA triple ionization. Once that is fixed, a least-squares fit to the experimental data gives the $f_{BR} = 0.222$ for the $2p$ IA triple ionization. In comparison, Kaastra & Mewe (1993) predicts that the branching ratio for a $2p$ hole to lead to triple ionization is zero. Here, there is also additional uncertainty because there is a large discrepancy between the triple-ionization measurements, with the cross section of Müller & Frodl (1980) being about 40% smaller than the results of Belic et al. (2010). For consistency, we have been using the Belic et al. data throughout this section.

For double ionization, there is good agreement between the Müller et al. (1985) and Belic et al. (2010) data. In order to describe Ar^{1+} double ionization, we adjust the branching ratios from Kaastra & Mewe (1993) downwards to account for the branching ratios that we empirically ascribe to triple and quadruple ionization. We then fit the data using Equations (2)

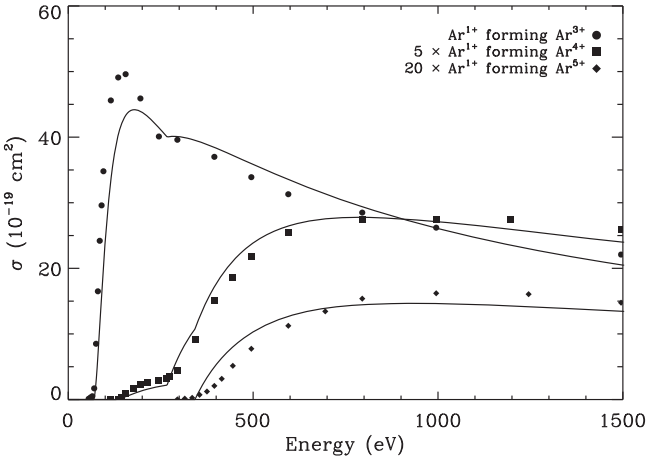

Figure 13. Double, triple, and quadruple ionization of Ar^{1+} forming Ar^{3+}, Ar^{4+}, and Ar^{5+}, respectively. The symbols show the data of Belic et al. (2010). For readability, the triple-ionization data were multiplied by a factor of 5 and the quadruple-ionization data by a factor of 20. Our cross sections using the semiempirical formulae are illustrated by the solid curves.

and (3) in order to determine the best value for p_0 in Equation (2), which we find to be $p_0 = 85.5$. The resulting cross section is compared to the experiments of Belic et al. (2010) in Figure 13. This value of p_0 disagrees with the one given by Shevelko et al. (2005), who found $p_0 = 67$, which was also based on Ar^{1+} measurements. The discrepancy may be due to our reducing the branching ratios for indirect processes in the Ar^{1+} double-ionization cross section. A value of $p_0 = 67$ does seem to be a good fit to double-ionization data for Cl^{0+} (Freund et al. 1990). To fit the data for Ti^{5+} or Fe^{9+}, we would require larger values of p_0, but this is consistent with other isoelectronic sequences where we found that Equations (2) and (3) become less predictive for $Z \geqslant 21$ ions. Instead, we can match the Ti^{5+} data using Equations (4) and (5) and the fits given by Shevelko et al. (2006). The Fe^{9+} measurements are well-described using Equation (1) with $f = 1$ plus Equation (6) for the IA contributions.

Based on the above results, we extrapolate the EIMI cross sections for other Cl-like ions in the following way: double ionization of ions with $Z \leqslant 20$ is described using Equations (2) and (3) with the parameters given in Shevelko et al. (2005). Double ionization of ions with $Z \geqslant 21$ uses Equation (1) with $f = 1$ and Equation (6). For triple ionization, we use Equation (1) with $f = 0.2$, as it is for all sequences from Na-like through Zn-like ions, and incorporate IA using Equation (6). Quadruple ionization is predicted by Equation (1) with $f = 1$ (as for all other Na-like through Ar-like isoelectronic sequences) and IA via the Lotz formula. For quintuple, sextuple, and septuple ionization, we also use Equation (1) with $f = 0.5$ for quintuple, $f = 0.2$ for sextuple, and $f = 0.07$ for septuple ionization. Since there is very little data on these processes, we apply the same scheme to all

Table 4
Inferred IA Branching Ratios for EIMI of Ar^{0+}

Subshell	Source	$\rightarrow Ar^{1+}$	$\rightarrow Ar^{2+}$	$\rightarrow Ar^{3+}$	$\rightarrow Ar^{4+}$	$\rightarrow Ar^{5+}$	$\rightarrow Ar^{6+}$	$\rightarrow Ar^{7+}$
$2p$	This work	0.0003	0.7497	0.25	0	0	0	0
$2p$	Kaastra & Mewe (1993)	0.0004	0.9997	0	0	0	0	0
$2s$	This work	0.0005	0.0361	0.4293	0.46	0.038	0	0
$2s$	Kaastra & Mewe (1993)	0.0005	0.0361	0.9634	0	0	0	0
$1s$	This work	0.0102	0.1172	0.1001	0.5172	0.1869	0.0544	0.014
$1s$	Kaastra & Mewe (1993)	0.0102	0.1172	0.1001	0.5172	0.2009	0.0544	0

quintuple, sextuple, and septuple EIMI of Cl-like through Zn-like isoelectronic sequences. For all of the above cases, except for argon, we use the Kaastra & Mewe (1993) branching ratios.

3.17. Ar-like

There is an extensive set of measurements for EIMI for Ar^{0+} from double to septuple ionization (Schram 1966; Krishnakumar & Srivastava 1988; Syage 1991; McCallion et al. 1992a; Almeida et al. 1994; Straub et al. 1995; Rejoub et al. 2002). As with the Cl-like ions above, we consider the data going backwards from septuple ionization and make empirical estimates for the indirect ionization branching ratios. Table 4 summarizes the inferred IA branching ratios for IA of Ar^{0+} and compares them to the original values from Kaastra & Mewe (1993).

Direct septuple ionization of Ar^{0+} forming Ar^{7+} can be described by Equation (1) with $f = 0.094$ at energies below the K-shell ionization threshold of about 3200 eV. For higher energies, we assume that the main indirect process is K-shell single ionization followed by sextuple autoionization, and that this can be represented using the Lotz formula multiplied by a branching ratio. A fit to the data of Schram (1966) implies a branching ratio of $f_{BR} = 0.014$. For comparison, Kaastra & Mewe (1993) predict no branching ratio for a net septuple ionization following a K-shell vacancy. Also, note that single ionization of an L-shell electron would not create a state with sufficient internal excitation to decay in a way that leads to septuple ionization; however, multiple ionization or excitation of the L-shell might contribute and we have not accounted for those effects.

Sextuple ionization can be described similarly, using Equation (1) with $f = 0.22$ and adding K-shell IA via the Lotz cross section with the branching ratio $f_{BR} = 0.0544$ from Kaastra & Mewe (1993). Here, the Kaastra & Mewe (1993) branching ratio appears reasonable. One issue with the sextuple-ionization data is that there is a large discrepancy between the measurements, with the cross section of Schram (1966) a factor of two larger than that of Almeida et al. (1994) below 2000 eV, which is the maximum energy measured by Almeida et al. (1994). Our fit lies in between these two measurements below 2000 eV, but matches the Schram (1966) results fairly well at higher energies.

The experimental quintuple-ionization threshold appears to be at least 100 eV above the theoretical DI threshold. The threshold corresponds well, instead, to that for single ionization of a $2s$ electron at ≈327 eV. This suggests that DI is negligible, although the measurements near the DI threshold are sparse. By fitting Equation (6) to the data, we estimate the IA branching ratio from $2s$ IA to be about $f_{BR} = 0.038$, but given the spread in the experimental measurements, the uncertainty is about a factor of two. We also add in K-shell IA using the Lotz cross section and the Kaastra & Mewe (1993) branching ratio adjusted down to 0.1869 to account for the branching ratio we ascribed to septuple ionization. Since we would like to estimate the cross sections for other systems that lack experimental data, it is useful to also fit these data using Equation (1). Doing so, we find that the magnitude of the data would be well-described with $f \approx 0.4$, although the threshold corresponds to the direct threshold and so is too low.

The measured quadruple-ionization threshold lies at ∼300 eV, well above the theoretical DI threshold of about 144 eV. Energetically, a $2p$ vacancy could lead to quadruple ionization, but the threshold matches better with the higher energy threshold for single ionization of the $2s$ subshell. A fit to the data using the Lotz cross section finds that the $2s$ IA branching ratio for quadruple ionization is $f_{BR} = 0.46$. To fully describe the cross section, we also add K-shell IA via the Lotz cross section multiplied by the Kaastra & Mewe (1993) branching ratio. Alternatively, the magnitude of the cross section could be approximately matched using Equation (1) with $f = 1$, but the threshold would be too low compared to experiment.

The direct triple ionization of Ar^{0+} forming Ar^{3+} exhibits a narrow peak that can best be fit using Equation (2) with $p_0 = 22.2$. For the indirect contributions, we use Equation (3). The branching ratios for $2s$ IA are adjusted down by about half from the Kaastra & Mewe (1993) branching ratios in order to account for the branching ratio we ascribe to higher-order EIMI. Then, we fit the data of Almeida et al. (1994) to find a $2p$ branching ratio of ≈0.25. The scatter in the various measured cross sections is roughly 20%.

Double ionization of Ar^{0+} is described using Equations (2) and (3). For the direct cross section, we find a best fit with $p_0 = 89.5$ in Equation (2). This is somewhat larger than the value of $p_0 = 80.0$ given by Shevelko et al. (2005). The reason for the discrepancy seems to be that Shevelko et al. based their fit on the data of Syage (1991), which are systematically low compared to various other measurements (see Figure 14). For the indirect cross sections, included via Equation (3), we use the Kaastra & Mewe (1993) branching ratios, with the $2p$ branching ratio reduced by 0.25 to account for the branching ratio we ascribed to triple ionization.

For double ionization of other Ar-like ions with $Z \leqslant 20$, we follow the same procedure and use Equation (2) with $p_0 = 89.5$ and Equation (3), but with the unmodified Kaastra & Mewe (1993) branching ratios. Comparing this scheme to the K^{1+} double EIMI data of Hirayama et al. (1986), we find that the DI part, i.e., Equation (2), matches quite well. However, we overestimate IA, which is probably because the Kaastra & Mewe (1993) predictions tend to underestimate the branching ratios for ejecting more electrons and therefore overestimate the branching ratios for ejecting fewer electrons (see Table 4). For double ionization of heavier ions, $Z \geqslant 21$, we estimate the

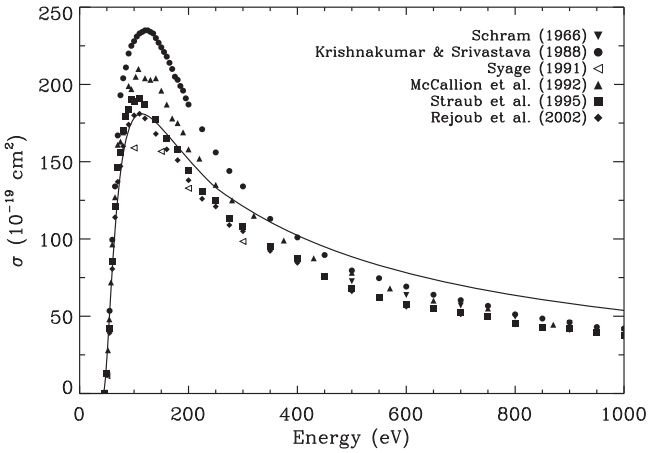

Figure 14. Double ionization of Ar^{0+} forming Ar^{2+}. The symbols show the data of Schram (1966, downward-pointing filled triangles), Krishnakumar & Srivastava (1988, filled circles), Syage (1991, open triangles), McCallion et al. (1992a, filled triangles), Straub et al. (1995, filled squares), and Rejoub et al. (2002, filled diamonds). Our fit, described in the text, is illustrated by the solid curve.

cross sections with Equation (1) with $f = 1$ and Equation (6) with the branching ratios from Kaastra & Mewe (1993).

The DI of other Ar-like ions is modeled by Equation (1) with $f = 0.2$ for triple ionization, $f = 1$ for quadruple ionization, $f = 0.5$ for quintuple ionization, $f = 0.2$ for sextuple ionization, and $f = 0.07$ for septuple ionization. For each of these ions, we also add IA contributions via the Lotz cross section and the Kaastra & Mewe (1993) branching ratios. We do not extrapolate our scaled branching ratios, because there is not enough data available to understand the variation of f_{BR} with Z within the isoelectronic sequence. In some cases, such as for quadruple and quintuple ionization, this scheme represents the same cross section as DI when in fact it is probably dominated by IA, as it is for Ar^{0+}. However, we lack a good method for extrapolating branching ratios. The above procedure is expected to at least estimate the magnitude of the cross sections, but the practical threshold is likely higher in energy than the DI threshold.

3.18. K-like through Zn-like

For ions in the K-like through Zn-like isoelectronic sequences, there are few data available to compare with. For this reason, we generally estimate the cross sections for ions in these isoelectronic sequences all following the same procedure. The exception is for those cases where there are experimental data, where we try to use the most accurate formulae even if they are not necessarily useful for predicting the behavior of other cross sections.

Shevelko et al. (2006) gives fits to experimental double-ionization cross sections for the low-charge states of Ti^{1-6+}, $Fe^{1,3-6+}$, and Ni^{1-6+} using Equations (4) and (5). For these ions, we use the Shevelko et al. (2006) fit parameters. We also use the same formulae to describe the Fe^{0+} data of Shah et al. (1993) with the fit parameters we found earlier (Hahn & Savin 2015a).

Measurements also exist for double ionization of Sc^{1+} (Jacobi et al. 2005) and Cu^{0+} (Freund et al. 1990; Bolorizadeh et al. 1994). Jacobi et al. (2005) found that Sc^{1+} measurements were well-described using Equation (1) for the direct cross section and adding to IA from ionization of a $3p$ electron using the Lotz cross section, i.e., Equation (6), with $f_{BR} = 0.68$. They find no contribution from the $3s$ IA. These inferred branching ratios are well below the predictions of Kaastra & Mewe (1993), who predict $f_{BR} = 1$ for IA arising from both $3s$ and $3p$ subshells. We find that the Cu data of Freund et al. (1990) and Bolorizadeh et al. (1994) can best be fit using Equation (2) with $p_0 = 10.44$ and using Equation (3) with the Kaastra & Mewe (1993) branching ratios for IA.

In order to predict the double-ionization cross sections of all unmeasured K-like through Zn-like systems, we take the predictions using Equation (1) with $f = 1$ and adding IA contributions via the Lotz formula and comparing to the cross sections reported by Shevelko et al. (2006). This method gives a reasonable alternative fit to these data, and so we used this procedure to estimate the cross sections for the unmeasured systems.

Triple ionization of Ti ions has been reported by Hartenfeller et al. (1998). We found that these triple-ionization cross sections could be described using Equation (1) plus IA through the Lotz cross section. In Equation (1), we find that for triple ionization, $f = 0.1$ fits K-like Ti^{3+}, $f = 0.2$ fits Ca-like Ti^{2+}, and $f = 0.25$ fits Sc-like Ti^{1+}.

Jacobi et al. (2005) measured triple-ionization of Sc^{1+} and found that the magnitude of the cross section was well-approximated by Equation (1), although the peak of the model cross section is broader than what was measured. Jacobi et al. also inferred a $2p$ IA branching ratio of $f_{BR} \approx 0.9$, which is in rough agreement with Kaastra & Mewe (1993). Based on their results, we represent the total Sc^{1+} triple-ionization cross section as a sum of the direct contribution using Equation (1) with $f = 1$ plus the indirect cross section using Equation (6) with branching ratios from Kaastra & Mewe (1993). This matches the measurements well near the threshold, but above about 400 eV, the cross section is overestimated by about 50%.

The Cu^{0+} triple-ionization measurements of Bolorizadeh et al. (1994) can be fit using the same scheme, setting $f = 0.16$ in Equation (1). In all cases, the IA branching ratios are from Kaastra & Mewe (1993). Based on these results, we estimate the triple-ionization cross sections for all other K-like through Zn-like ions using the same procedure and setting $f = 0.2$ in Equation (1).

Quadruple ionization can also be described using Equation (1) plus the indirect contributions using Equation (6) with the branching ratios from Kaastra & Mewe (1993). For Ti^{1+} (Hartenfeller et al. 1998), we find $f = 0.25$ in Equation (1), while for Cu^{0+} (Bolorizadeh et al. 1994), $f = 0.1$. Jacobi et al. (2005) found that their quadruple-ionization measurements of Sc^{1+} could be matched by using $f = 0.15$ in Equation (1) and branching ratios of $f_{BR} = 0.02$ for $2p$ IA and $f_{BR} = 0.8$ for $2s$ IA. Since their estimated branching ratios are very close to the predictions of Kaastra & Mewe (1993), we continue to use the Kaastra & Mewe results in our compilation.

For ions that have not been measured, we err on the conservative end of the estimated f values for Equation (1) and set $f = 0.1$ in estimating the direct quadruple-ionization cross sections for other ions in these isoelectronic sequences. We model the indirect cross sections as IA using the Lotz cross section and Kaastra & Mewe (1993) branching ratios.

Quintuple-ionization measurements for these isoelectronic sequences have been performed only for Sc^{1+} (Jacobi et al. 2005) and Cu^{0+} (Bolorizadeh et al. 1994). For Sc^{1+}, Jacobi et al. (2005) found that the measurements could be

matched up to about 590 eV using Equation (1) with $f = 0.008$ plus IA represented by the Lotz cross section with $f_{BR} = 0.0006$ for the $2p$ subshell and 0.055 for the $2s$ subshell. Above 590 eV, they found additional indirect ionization cross sections, which they ascribed to a MIMA process involving direct double ionization of inner-shell electrons followed by autoionization of three additional electrons. Since it is difficult to model these complex ionization processes given the limited available data, we represent the Sc^{1+} quintuple-ionization cross section using Equation (1) with $f = 0.5$, which matches the peak of the experimental data but overestimates the cross section between the DI threshold at ≈313 eV and the onset of unknown ionization processes at 590 eV.

For Cu^{0+}, the quintuple-ionization cross section is well-described by Equation (1) with $f = 0.65$ and adding in IA contributions using Equation (6) multiplied by the branching ratios from Kaastra & Mewe (1993). Based on this, and also considering our quintuple-ionization results for Ar-like and Cl-like ions, we estimate all other quintuple-ionization cross sections using the same scheme, but with $f = 0.5$ in Equation (1).

As far as we know, there are no sextuple- or septuple-ionization measurements for K-like through Zn-like ions. Based on our results for Ar-like and Cl-like ions, we estimate these cross sections using Equations (1) and (6) multiplied by the IA branching ratios. For Equation (1), we set $f = 0.2$ for sextuple ionization and $f = 0.07$ for septuple ionization.

In some cases, Kaastra & Mewe (1993) predict branching ratios for higher-order EIMI beyond septuple ionization. In those cases, we only use Equation (6) multiplied by the Kaastra & Mewe branching ratios. Because DI contributions are likely to be small and there are no data, we ignore DI for EIMI beyond septuple ionization.

3.19. Uncertainties

Given the sparseness of experimental EIMI data with which to compare, it is difficult to quantitatively describe their uncertainty. Nevertheless, we can give at least some rough estimate for the accuracy of our interpolations. For double ionization, there are data for most isoelectronic sequences and the semiempirical formulae seem to perform quite well. On this basis, we would estimate our double-ionization cross sections to be accurate to ∼30%. There is significantly less data available for triple ionization, and our cross sections are probably accurate to about a factor of two or better. For higher-order EIMI, our estimates are essentially guesses, and we can only say that they are probably within an order of magnitude.

For many quadruple- and higher-order EIMI cross sections, we estimated the cross sections using Equation (1), which is a scaling for DI. These estimates are adequate for matching the magnitude of the cross sections in the limited available data. However, indirect processes are probably more important than DI, and this scheme probably understates the effective energy threshold. For plasmas where the electron distribution includes many electrons below the true effective energy threshold, our estimates may have the effect of generating too high of a rate coefficient for the corresponding ionization process.

4. Summary and Future Needs

We report the first comprehensive set of EIMI cross sections for the astrophysically relevant He-like through Zn-like systems. These data will be useful for the modeling of collisionally ionized plasmas that are subject to rapid heating or that have non-thermal electron distributions. Up to now, the lack of EIMI data has led most researchers to ignore EIMI. Our data can be used to quantify the effect of EIMI in the modeling of astrophysical systems. The application of these kinds of data can be expected to grow as the precision of astrophysical diagnostics requires increasingly precise atomic data for interpretation.

In reviewing the data, we used semiempirical formulae and identified some of their limitations. Equation (1) tends to overestimate the EIMI cross section and so we introduced a scaling factor $f < 1$ in order to match the experimental data. We often resort to this formula for describing triple- and higher-order EIMI because it appears to predict the magnitude well, although it does not account for IA processes, which can dominate those cross sections. As a result, this formula can significantly underestimate the effective EIMI threshold, which is often higher than the DI threshold.

In some cases also, the shape of the cross section predicted by Equation (1) does not match the data very well, particularly near the peak cross section. For example, the sharp peaks in the direct triple-ionization data for N^{1+}, Ne^{0+}, and Ar^{0+} are better matched by a fit based on Equation (2), which was developed for direct double ionization. It appears that this problem is prevalent for near-neutrals, but this may be only an experimental bias since most of the existing triple-ionization experiments are for neutrals and singly charged ions.

We found that Equation (2) works very well for describing direct double ionization of light ions ($Z \leqslant 20$), though with some caveats. For near-neutrals, we found that it is usually necessary to reduce the p_0 value from that given by Shevelko et al. (2005). For heavier ions ($Z \geqslant 21$), the parameter p_0 varies significantly within the isoelectronic sequence so that the formula is no longer predictive, and we use instead Equation (1) with the parameters of Bélenger et al. (1997).

IA is included in our cross sections by using either Equations (3) or (6). Generally, we use Equation (3) when DI is described by Equation (2) and we use the Lotz formula, i.e., Equation (6), when DI is described by Equation (1). In either case, the cross sections are scaled by the branching ratios f_{BR}, for which we have relied mainly on Kaastra & Mewe (1993). For some cases, we were able to infer f_{BR} from the data and compare to the predictions of Kaastra & Mewe. Our comparison shows that Kaastra & Mewe tend to underestimate the branching ratios for ejecting many electrons and so overestimate the branching ratios for ejecting fewer electrons (see Tables 3 and 4).

A systematic factor that may contribute to the discrepancy between the theoretical and experimental IA branching ratios is the effect of excitation during the initial collision. Kučas et al. (2015) calculated autoionization branching ratios for K-shell vacancies for various charge states of Ne, Mg, Si, S, and Ar. In their calculations, they included the ground configuration with a K-shell vacancy as well as excited configurations that had both a K-shell vacancy plus additional excitation. For the ground configurations, the Kučas et al. (2015) branching ratios are very similar to the results of Kaastra & Mewe (1993). However, when the initial configuration is more excited, there

	0	1	2	3	4	5	6	7	8	9	10	11	12	13	14	15	16	17	18	19	20	21	22	23	24	25	26	27	28
He	X																												
Li	X	X																											
Be																													
B		X																											
C		X	X	X																									
N		X	X	X	X																								
O	X	X		X	X																								
F		X																											
Ne	X	X	X	X	X	X	X																						
Na	X	X																											
Mg	X																												
Al		X	X	X	X																								
Si	X																												
P	X																												
S	X																												
Cl	X																												
Ar	X	X	X	X	X	X	X	X	X	X	X	X																	
K		X																											
Ca																													
Sc		X																											
Ti		X	X	X	X	X	X																						
V																													
Cr																													
Mn																													
Fe	X	X		X	X	X	X			X		X		X															
Co																													
Ni		X	X	X	X	X	X				X	X	X	X	X	X													
Cu	X																												
Zn																													

Figure 15. Chart summarizing the availability of double-ionization data for various ions. The elements are given in rows, and each column represents the initial charge state for the reaction, e.g., He^{0+} is represented by the top-left corner of the table. The astrophysically abundant elements, He, C, N, O, Ne, Mg, Si, S, Ar, Ca, Fe, and Ni, are highlighted in bold. An "X" in the corresponding box indicates that experimental double-ionization data exist for the reaction. Note that isoelectronic sequences fall on the diagonals. The references for these experimental data can be found in Table 1.

are substantial branching ratios for the ejection of additional electrons. Thus, if an electron–ion collision leads to excitation in addition to the ionization of a core electron, the branching ratio for higher-order EIMI processes can be higher than predicted based on the Kaastra & Mewe branching ratios. Unfortunately, it is not feasible to perform a detailed comparison of the Kučas et al. (2015) predictions with the available EIMI cross sections. This is because for the ions that have branching ratio calculations, the EIMI measurements are most detailed at low energies, below the K-shell IA threshold, and because the cross sections are dominated by L-shell IA so that the K-shell IA is small and not well resolved.

Because of the limited available experimental data and the lack of reliable theory, we expect that these estimated cross sections will need to be revised in the future. Currently, double-ionization measurements are the most comprehensive, but even for double ionization there are few measurements for high-charge states or for heavy ions. For higher-order EIMI, the dearth of experimental data is much worse. For many isoelectronic sequences, such as Be-like, O-like, Al-like, Si-like, and P-like, we could not find any triple-ionization measurements. Most isoelectronic sequences lack any measurements of quadruple- or higher-order EIMI.

The lower-order EIMI cross sections are the largest, with the magnitude of the cross sections typically falling by an order of magnitude for each additional ejected electron. Thus, the lower-order EIMI cross sections are expected to be the most important and it would make sense to prioritize measurements of double and triple ionization to fill in the existing gaps.

One limitation of the existing data for double and triple ionization is that the measured systems are generally for light and/or low-charge ions. For example, we are not aware of any double-ionization measurements for He-like through C-like ions from ions heavier than neon. For M-shell ions, most of the double-ionization data come from neutral species or from argon ions. These deficiencies in the double-ionization database are illustrated graphically in Figures 15 and 16. For triple ionization, we are not aware of any measurements where the

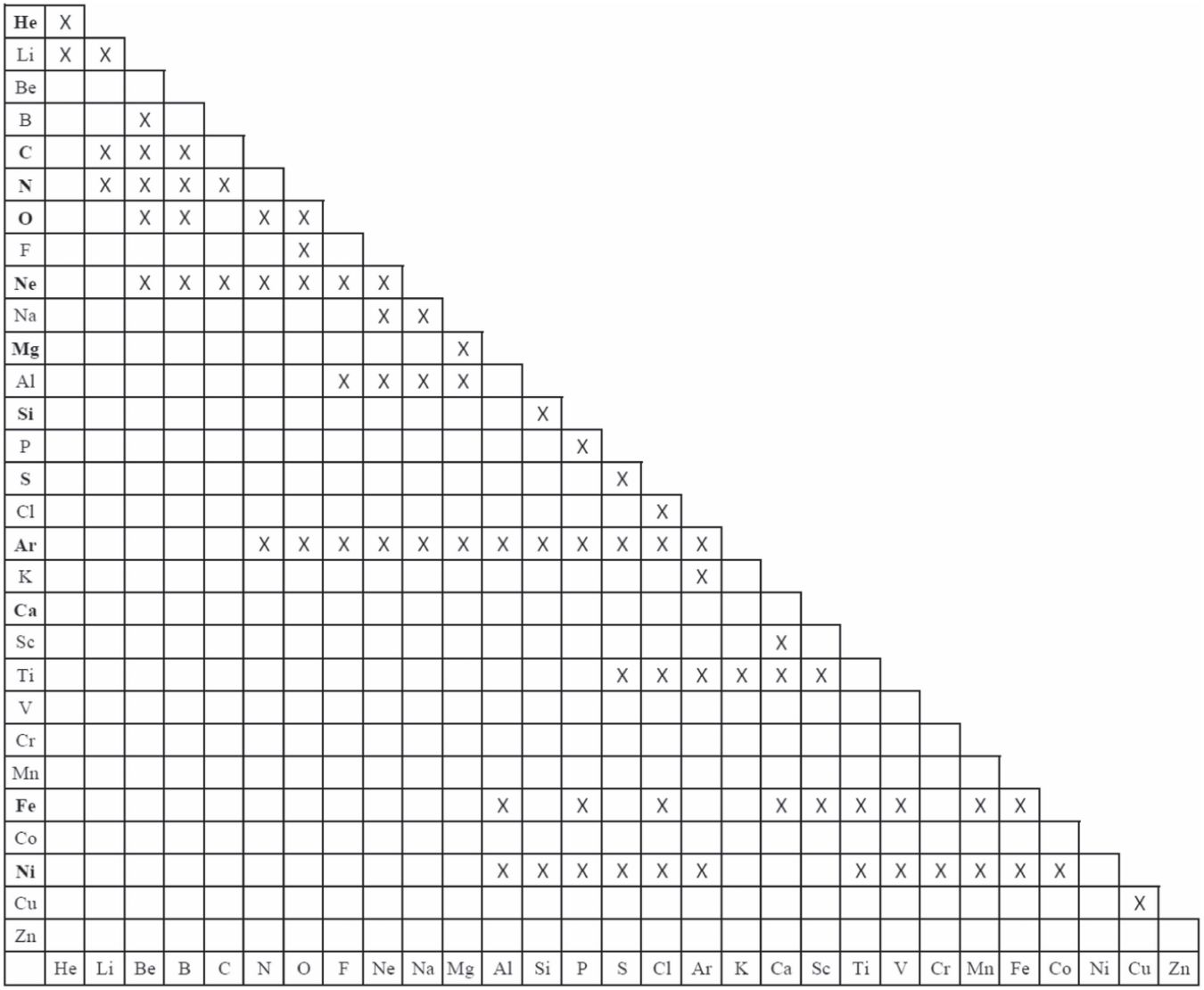

Figure 16. Same as Figure 15, except that here the columns label isoelectronic sequences.

initial ion is more than three times ionized. In order to understand how these cross sections evolve along isoelectronic sequences, data are needed for heavier and more highly charged ions.

The theoretical problem of EIMI is difficult to address because it is a complex many-body problem. However, one advance that could significantly affect the EIMI data would be a revision of the Kaastra & Mewe (1993) IA branching ratios, i.e., the calculation of the probability distribution of the number of ejected electrons following inner-shell single ionization. IA is the dominant ionization process for highly charged ions and for high-order EIMI. The atomic structure calculations upon which the Kaastra & Mewe data are based are more than 50 years old. Revising these data should be a tractable theoretical problem. It would also be interesting and useful to calculate similar branching ratios for multiple vacancies and excited states.

This work was supported in part by the NASA Living with a Star Program grant NNX15AB71G and by the NSF Division of Atmospheric and Geospace Sciences SHINE program grant AGS-1459247.

Appendix A
Maxwellian Rate Coefficients

For some plasma applications, it is often convenient to have Maxwellian plasma rate coefficients rather than cross sections. We derived such rate coefficients from our estimated cross sections using the following procedure (see also Hahn et al. 2011a). Each partial EIMI cross section, as given by each row of Table 2, was multiplied by the electron–ion relative velocity and integrated over a Maxwellian velocity distribution to obtain a partial EIMI rate coefficient $\alpha_I(T_e)$ as a function of electron temperature T_e (Müller 1999). The total rate coefficient is the sum of all relevant partial rate coefficients. Fogle et al. (2008) showed that accurate rate coefficients are obtained by carrying out the integration over an energy range from the EIMI threshold for each partial cross section, E_{th}, up to $E_{th} + 6k_BT_e$, where k_B is the Boltzmann constant. Our calculations considered a temperature range of $T_e = 10^4$–10^9 K.

In order to tabulate the partial EIMI rate coefficients, we scaled them to a form that can be reliably fit by a polynomial. The polynomial coefficients a_i can be used to reproduce the scaled rate coefficient $\rho(x)$ as a function of the scaled

Table 5
Fitting Parameters for Maxwellian Rate Coefficients

Z	q_i	q_f	E_{th} (eV)	a_0	a_1	a_2	a_3	a_4	a_5	a_6	a_7	Max Rel. Error
2	0	2	79.0052	0.0076421	0.154173	1.7303	−7.29139	12.8955	−11.0427	3.53095	0	0.0281082
3	0	2	81.0318	0.000725418	1.58424	−5.80349	12.6638	−16.7906	12.188	−3.88502	0	0.0247008
3	0	3	203.486	−1.08E–06	0.00223967	−0.00541118	0.0134891	−0.0218751	0.0198431	−0.00745306	0	0.015704
3	1	3	198.094	0.0043405	0.0914753	0.963979	−4.04111	7.07208	−5.99096	1.88956	0	0.0296052
4	0	2	27.5339	0.00188238	1.41033	−4.96733	10.2226	−12.6706	8.59098	−2.619	0	0.0191486
4	0	2	123.63	2.87337	36.7149	−264.598	965.423	−1789.41	1642.95	−598.184	0	0.109417
4	1	3	172.107	0.00111361	1.53842	−5.64993	12.4687	−16.8623	12.5446	−4.08705	0	0.0123538
4	2	4	371.615	0.00184752	0.0877745	0.466093	−2.07169	3.58873	−2.99769	0.915397	0	0.0196791

(This table is available in its entirety in machine-readable form.)

temperature x using

$$\rho(x) = 10^{-6}\sum_i a_i x^i. \quad (8)$$

The EIMI plasma rate coefficient in units of $cm^3\,s^{-1}$ as a function of electron temperature $\alpha_I(T_e)$ is calculated from ρ using (Dere 2007; Hahn 2014)

$$\alpha_I(T_e) = t^{-1/2}E_{th}^{-3/2}E_1(1/t)\rho(x), \quad (9)$$

where $E_1(1/t)$ is the first exponential integral and $t = k_B T_e/E_{th}$. The scaled temperature x is given by

$$x = 1 - \frac{\ln 2}{\ln(t+2)}. \quad (10)$$

This expression can be inverted to obtain T_e from x as

$$T_e = \frac{E_{th}}{k_B}\left[\exp\left(\frac{\ln 2}{1-x}\right) - 2\right]. \quad (11)$$

Thus, the procedure for calculating each partial rate coefficient $\alpha_I(T_e)$ from the fitting parameters is to first use Equation (10) to get the scaled temperature x corresponding to T_e, then calculate $\rho(x)$ from the polynomial fit parameters with Equation (8), and finally de-scale $\rho(x)$ using Equation (9) to find $\alpha_I(T_e)$. If the total EIMI rate coefficient is desired, it can be obtained by summing all of the partial rate coefficients sharing the same initial and final charge states.

Fitting coefficients are reported in a machine-readable table, a sample of which is illustrated by Table 5. The first four columns of the table give the nuclear charge Z, initial charge state q_i, final charge state q_f, and EIMI threshold E_{th}, followed by the polynomial fit coefficients a_i. The final column of the table is the fractional maximum relative error of the polynomial fit compared to the calculated rate coefficient in the temperature range where α_I is non-negligible, defined as $\alpha_I > 10^{-30}$ $cm^3\,s^{-1}$. The maximum errors in the fit tend to be at low T_e, where α_I is smallest. The median maximum error of the polynomial fits is about 2.5% and the fits are generally better than 10%. This error represents only the quality of the polynomial fit and does not include any physical uncertainties, such as those discussed in the body of this paper.

Finally, we emphasize that these rate coefficients are appropriate only for Maxwellian plasmas. We anticipate that many of the most significant applications of these EIMI data will be for non-Maxwellian plasmas, such as kappa distributions. For such plasmas, appropriate rate coefficients can sometimes be approximated based on the Maxwellian rate coefficients (e.g., Hahn & Savin 2015b). However, for non-Maxwellian distributions, it would be preferable to directly calculate the non-Maxwellian rate coefficients by carrying out the integration of the cross section over the appropriate velocity distribution.

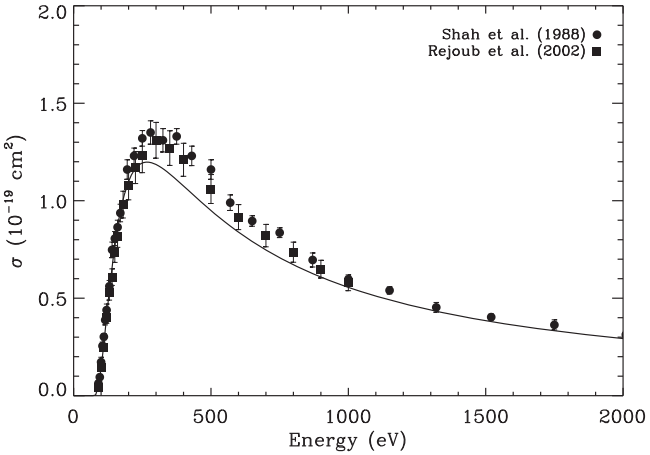

Figure 17. Fit compared to the EIMI data for He^{0+} forming He^{2+}.
(The complete figure set (86 images) is available.)

Appendix B
Examples

Here we provide a more extensive set of examples showing our cross sections compared to EIMI measurements. Figure 17 is not comprehensive, as we only plotted those fits for which we have a tabulation of the experimental data. In some cases, data were not tabulated in the original references. For example, the double-ionization data for low-charge states of Ti, Fe, and Ni were not available in tabular form, and our parameters are based on the fits provided by Shevelko et al. (2006). In other such cases, our fits are based on a careful inspection of the figures in the experimental papers, e.g., triple ionization of Ti^{1+}, Ti^{2+}, and Ti^{3+} as reported by Hartenfeller et al. (1998).

In most cases, we include error bars on the experimental data in these figures. However, error bars are suppressed in cases where there are many data points (e.g., double ionization Ar^{0+}), else the plot would be too cluttered, and whenever the uncertainties are not tabulated in the experimental references. In the latter cases, the experimental papers usually provide a general discussion of the uncertainties in the text. For example,

Freund et al. (1990) do not tabulate uncertainties, but give a discussion in the text estimating a general uncertainty level of about 10% on their absolute cross sections.

References

Akahori, T., & Yoshikawa, K. 2010, PASJ, 62, 335
Almeida, D. P., Fontes, A. C., & Godinho, C. F. L. 1995, JPhB, 28, 3335
Almeida, D. P., Fontes, A. C., Mattos, I. S., & Godinho, C. L. 1994, JESRP, 67, 503
Bautista, M. A., Mendoza, C., Kallman, T. R., & Palmeri, P. 2003, A&A, 403, 339
Bélenger, C., Defrance, P., Salzborn, E., et al. 1997, JPhB, 30, 2667
Belic, D. S., Falk, R. A., Timmer, C., & Dunn, G. H. 1987, PhRvA, 36, 1073
Belic, D. S., Lecointre, J., & Defrance, P. 2010, JPhB, 43, 185203
Berakdar, J. 1996, PhLA, 220, 237
Boivin, R. F., & Srivastava, S. K. 1998, JPhB, 31, 2381
Bolorizadeh, M. A., Patton, C. J., Shah, M. B., & Gilbody, H. B. 1994, JPhB, 27, 175
Bradshaw, S. J., & Klimchuk, J. A. 2011, ApJS, 194, 26
Bryans, P., Badnell, N. R., Gorczyca, T. W., et al. 2006, ApJS, 167, 343
Bryans, P., Landi, E., & Savin, D. W. 2009, ApJ, 691, 1540
Cherkani-Hassani, S., Defrance, P., & Oualim, E. M. 1999, PhST, 80, 292
Cherkani-Hassani, S., Khouilid, M., & Defrance, P. 2001, PhST, 92, 287
Defrance, P., Kereselidze, T. M., & Machavariani, Z. S. 2003, NIMPB, 205, 405
Defrance, P., Kereselidze, T. M., Machavariani, Z. S., & Noselidze, I. L. 2000, JPhB, 33, 4323
Dere, K. P. 2007, A&A, 466, 771
Duponchelle, M., Khouilid, M., Oualim, E. M., Zhang, H., & Defrance, P. 1997, JPhB, 30, 729
Fisher, V., Ralchenko, Y., Goldgirsh, A., Fisher, D., & Maron, Y. 1995, JPhB, 28, 3027
Fogle, M., Bahati, E. M., Bannister, M. E., et al. 2008, ApJS, 175, 543
Freund, R. S., Wetzel, R. C., Shul, R. J., & Hayes, T. R. 1990, PhRvA, 41, 3575
Garcia, J., Kallman, T. R., Witthoeft, M., et al. 2009, ApJS, 185, 477
Gorczyca, T. W., Dumitriu, I., Hasoğlu, M. F., et al. 2006, ApJ, 638, 121
Gorczyca, T. W., Kodituwakku, C. N., Zatsarinny, O., et al. 2003, ApJ, 592, 636
Götz, J. R., Walter, M., & Briggs, J. S. 2006, JPhB, 39, 4365
Gryziński, M. 1965, PhRv, 138, 336
Hahn, M. 2014, J. Phys. Conf. Ser., 488, 012050
Hahn, M., Becker, A., Bernhardt, D., et al. 2013, ApJ, 767, 47
Hahn, M., Becker, A., Grieser, M., et al. 2012, ApJ, 760, 80
Hahn, M., Bernhardt, D., Grieser, M., et al. 2011a, ApJ, 729, 76
Hahn, M., Grieser, M., Krantz, C., et al. 2011b, ApJ, 735, 105
Hahn, M., & Savin, D. W. 2015a, ApJ, 800, 68
Hahn, M., & Savin, D. W. 2015b, ApJ, 809, 178
Hartenfeller, U., Aichele, K., Hathiramani, D., et al. 1998, JPhB, 31, 3013
Hasoğlu, M. F., Gorczyca, T. W., Korista, K. T., et al. 2006, ApJL, 649, L149
Hirayama, T., Oda, K., Morikawa, Y., et al. 1986, JPSJ, 55, 1411
Huang, M.-T., Wong, W. W., Inokuti, M., Southworth, S. H., & Young, L. 2003, PhRvL, 90, 163201
Huang, M.-T., Zhang, L., Hasegawa, S., Southworth, S. H., & Young, L. 2002, PhRvA, 66, 012715
Jacobi, J., Knopp, H., Schippers, S., Shi, W., & Müller, A. 2005, JPhB, 38, 2015
Jalin, R., Hagermann, R., & Botter, R. 1973, JChPh, 59, 952
Jonauskas, V., Prancikevičius, A., Masys, Š, & Kynienė, A. 2014, PhRvA, 89, 052714
Kaastra, J. S., & Mewe, R. 1993, A&AS, 97, 443
Kim, Y.-K., & Rudd, M. E. 1994, PhRvA, 50, 3954
Kim, Y.-K., Santos, J. P., & Parente, F. 2000, PhRvA, 62, 052710
Kramida, A., Ralchenko, Y., Reader, J. & NIST ASD Team 2016, NIST Atomic Spectra Database, v.5.4 (Gaithersburg, MD: National Institute of Standards and Technology), https://physics.nist.gov/asd
Krishnakumar, E., & Srivastava, S. K. 1988, JPhB, 21, 1055
Kučas, S., Momkauskaite, A., & Karazija, R. 2015, ApJ, 810, 26
Lahmam-Bennani, A., Staicu Casagrande, E. M., Naja, A., Dal Cappello, C., & Bolognesi, P. 2010, JPhB, 43, 105201
Lebius, H., Binder, J., Koslowski, H. R., Wiesemann, K., & Huber, B. A. 1989, JPhB, 22, 83
Lecointre, J., Kouzakov, K. A., Belic, D. S., et al. 2013, JPhB, 46, 205201
Lotz, W. 1969, ZPhy, 220, 466
Magee, N. H., Abdallah, J., Jr., Clark, R. E. H., et al. 1995, in ASP Conf. Ser. 78, Astrophysical Applications of Powerful New Databases, ed. S. J. Adelman & W. L. Wiese (San Francisco, CA: ASP), 51
McCallion, P., Shah, M. B., & Gilbody, H. B. 1992a, JPhB, 25, 1061
McCallion, P., Shah, M. B., & Gilbody, H. B. 1992b, JPhB, 25, 1051
Mendoza, C., Kallman, T. R., Bautista, M. A., & Palmeri, P. 2004, A&A, 414, 377
Müller, A. 1986, PhL, 113A, 415
Müller, A. 1999, IJMSp, 192, 9
Müller, A. 2005, NIMPB, 233, 141
Müller, A. 2008, in Advances in Atomic, Molecular, and Optical Physics, Vol. 55, ed. E. Arimondo, P. Berman, & C. Lin (London: Elsevier), 293
Müller, A., Bernhardt, D., Borovik, A., Jr., et al. 2017, ApJ, 836, 166
Müller, A., & Frodl, R. 1980, PhRvL, 44, 29
Müller, A., Tinschert, K., Achenbach, C., Becker, R., & Salzborn, E. 1985, JPhB, 18, 3011
Müller, A., Tinschert, K., Hofmann, G., Salzborn, E., & Dunn, G. H. 1988, PhRvL, 61, 70
Palmeri, P., Mendoza, C., Kallman, T. R., Bautista, M. A., & Meléndez, M. 2003, A&A, 410, 359
Palmeri, P., Quinet, P., Mendoza, C., et al. 2011, A&A, 525, 59
Palmeri, P., Quinet, P., Mendoza, C., et al. 2012, A&A, 543, 44
Patnaude, D. J., Ellison, D. C., & Slane, P. 2009, ApJ, 696, 1956
Peart, B., & Dolder, K. T. 1969, JPhB, 2, 1169
Pindzola, M. S., Ballance, C. P., Robicheaux, F., & Colgan, J. 2010, JPhB, 43, 105204
Pindzola, M. S., & Loch, S. D. 2017, JPhB, 50, 085203
Pindzola, M. S., Ludlow, J. A., Ballance, C. P., Robicheaux, F., & Colgan, J. 2011, JPhB, 44, 105202
Pindzola, M. S., Ludlow, J. A., Robicheaux, F., Colgan, J., & Griffin, D. C. 2009, JPhB, 42, 215204
Rachafi, S., Belic, D. S., Duponchelle, M., et al. 1991, JPhB, 24, 1037
Reale, F., & Orlando, S. 2008, ApJ, 684, 715
Rejoub, R., Lindsay, B. G., & Stebbings, R. F. 2002, PhRvA, 65, 042713
Schram, B. L. 1966, Phy, 32, 197
Schram, B. L., Boerboom, A. J. H., & Kistemaker, J. 1966, Phy, 32, 185
Shah, M. B., Elliot, D. S., McCallion, P., & Gilbody, H. B. 1988, JPhB, 21, 2751
Shah, M. B., McCallion, P., Okuno, K., & Gilbody, H. B. 1993, JPhB, 26, 2393
Shevelko, V. P., & Tawara, H. 1995a, PhyS, 52, 649
Shevelko, V. P., & Tawara, H. 1995b, JPhB, 28, L589
Shevelko, V. P., Tawara, H., Scheuermann, F., et al. 2005, JPhB, 38, 525
Shevelko, V. P., Tawara, H., Tolstikhina, I. Y., et al. 2006, JPhB, 39, 1499
Steidl, M., Aichele, K., Hartenfeller, U., et al. 1999, in Proc. 21st Int. Conf. Physics of Photonic, Electronic, and Atomic Collisions, ed. Y. Itikawa et al. (Singapore: World Scientific), 362
Stenke, M., Hartenfeller, U., Aichele, K., et al. 1999, JPhB, 32, 3641
Stenke, M., Hathiramani, D., Hofmann, G., et al. 1995, NIMPB, 98, 138
Stolte, W. C., Jonauskas, V., Lindle, D. W., Sant'Anna, M. M., & Savin, D. W. 2016, ApJ, 818, 149
Straub, H. C., Renault, P., Lindsay, B. G., Smith, K. A., & Stebbings, R. F. 1995, PhRvA, 52, 1115
Syage, J. A. 1991, JPhB, 24, 527
Talukder, M. R., Haque, A. K. F., & Uddin, M. A. 2009, EPJD, 53, 133
Tate, J. T., & Smith, P. T. 1934, PhRv, 46, 773
Thompson, W. R., Shah, M. B., & Gilbody, H. B. 1995, JPhB, 28, 1321
Tinschert, K. 1989, PhD thesis, Justus-Liebig Universität Giessen
Tinschert, K., Müller, A., Phaneuf, R. A., Hofmann, G., & Salzborn, E. 1989, JPhB, 22, 1241
Westermann, M., Scheuermann, F., Aichele, K., et al. 1999, PhyS, T80, 285
Yu, D. J., Rachafi, S., Jureta, J., & Defrance, P. 1992, JPhB, 25, 4593
Zambra, M., Belic, D., Defrance, P., & Yu, D. J. 1994, JPhB, 27, 2383
Zhang, H., Cherkani-Hassani, S., Bélenger, C., et al. 2002, JPhB, 35, 3829
Ziegler, D. L., Newman, J. H., Goeller, L. N., Smith, K. A., & Stebbings, R. F. 1982a, P&SS, 30, 1269
Ziegler, D. L., Newman, J. H., Smith, K. A., & Stebbings, R. F. 1982b, P&SS, 30, 451